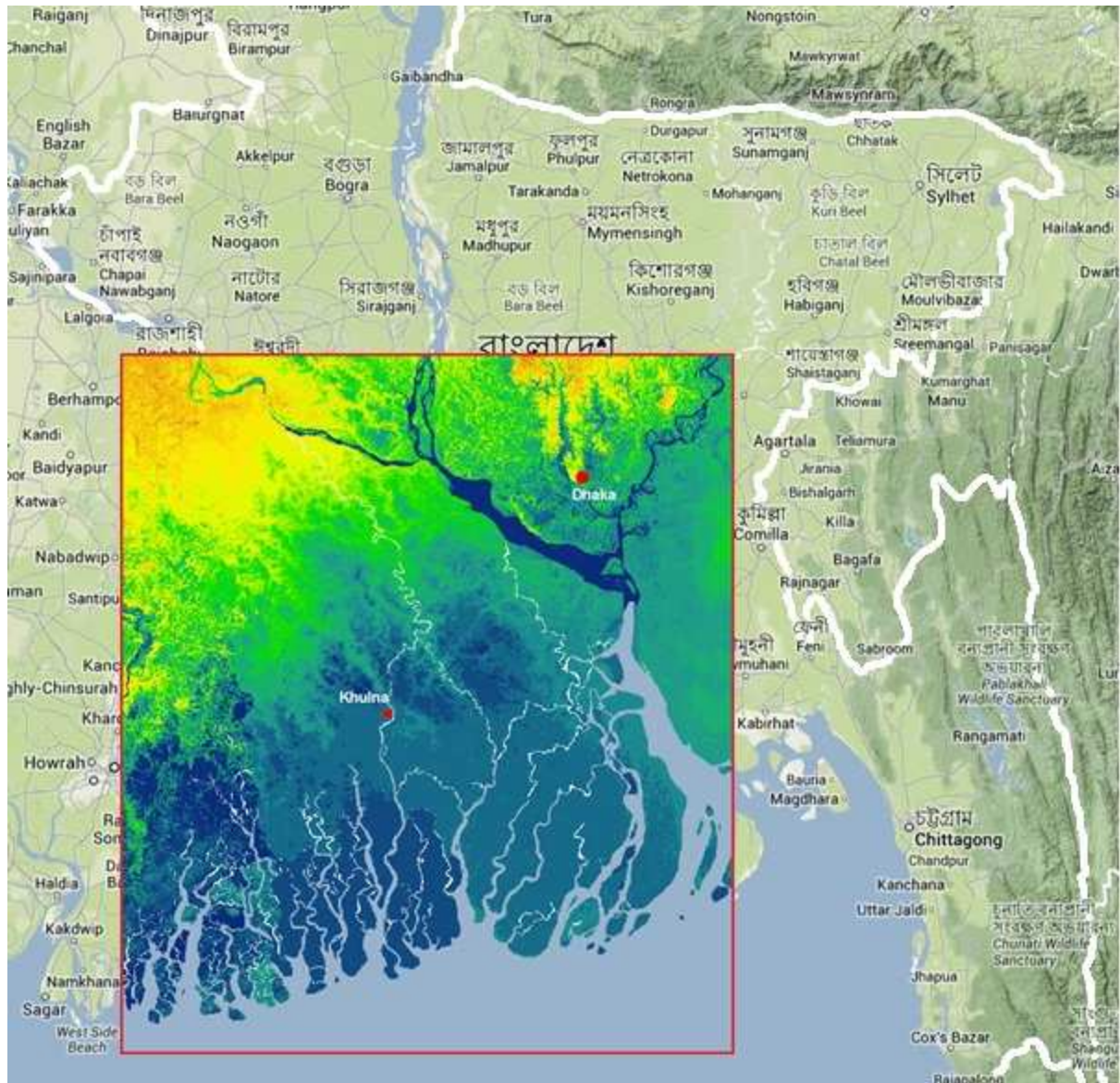# SWIBANGLA: Managing salt water intrusion impacts in Bangladesh

Dataset, data processing and model input

Master Internship

Marjolein Vogels

Supervisor UU: Prof. M. Bierkens

Supervisors Deltares: Marta Faneca Sanchez,

Gijs Janssen, Gualbert Oude Essink

Utrecht University
Faculty of Geosciences
Department of Physical Geography

Deltares
Unit: Bodem- en Grondwatersystemen
Department: Grondwaterbeheer

Cover: Bangladesh and the SWIBANGLA model domain

January, 2014

Contents

APSU: Arsenic Policy Support Unit

BADC: Bangladesh Agricultural Development Cooperation

BGS: British Geological Survey

BMD: Bangladesh Meteorological Department

BWDB: Bangladesh Water Development Board

CEGIS: Center for Environmental and Geographic Information Services

DPHE: Department of Public Health and Engineering

EPC: Engineering and Planning Consultants (Dhaka)

GoB: Government of the People's Republic of Bangladesh

HTS: Hunting Technical Services

JICA Bangladesh: Japan International Cooperation Agency

MMI: Mot MacDonald International

MMP: M. MacDonald and Partners (UK)

UNICEF: United Nations Children's Fund

WB: World Bank

List of figures

List of Tables

Preface

Bangladesh is located on the Northern coast of the Bay of Bengal in South Asia and its geography is majorly characterized by the delta of the Ganges and the Brahmaputra. Tropical monsoons, frequent floods and cyclones occur frequently in this low-lying area. The combination of enhanced anthropogenic activity and climate change increases the pressure on its coastal groundwater system and increases the magnitude of salt water intrusion. This can quickly become the second environmental and health threat next to the well-known and studied mass arsenic poisoning that this country suffers.

Within the BRAC WASH II program the SWIBANGLA project was launched, which aims to update current water safety plans to manage salt water intrusion impacts in Bangladesh. Part of this project is to create a 3D numerical variable-density and solute transport model of the coastal groundwater system in Bangladesh using SEAWAT. This is pursued by collecting existing knowledge and data and analysis of the water system. After calibration and simulation of the model, several impact studies are assessed by this model, for example a rising sea level. Mitigation techniques are implemented in the model to counteract these impacts and their effects and efficiency are assessed. The model will give a better understanding in the water fluxes and solute transport of the Bangladesh coastal groundwater system and will provide a tool in monitoring the system and identifying potential risks. It will also give insight in how several mitigation techniques can be applied to sustain a climate-proof fresh groundwater supply and reduce salt water intrusion.

The aim of this internship is to create this 3D fresh-salt model and to deliver this as a product. This report is an overview of the model set-up and it contains information about the dataset, data processing and model building. The current state of the model is that of fine-tuning the water balances and the fresh-salt distribution. A big part of this internship went into the discussion about how to make a scarce dataset representative and model proof. This was both challenging and fun. Not everywhere are datasets as extensive and open access as in the Netherlands or other western countries. Another part of the SWIBANGLA project was to invite a Bangladeshi from CEGIS at Deltares to help accessing and retrieving data from organizations in Bangladesh, but it was also seen as a capacity building program to develop the individual research capability of young professionals. This task was also partly assigned to me and it was definitely an interesting and a valuable experience to share information about numeric groundwater modeling with someone from such a different culture and education environment. Also an adapted SEAWAT code is created within Deltares to make SEAWAT groundwater models more accessible, understandable and readable from a client's perspective. This software is used and tested for the SWIBANGLA model, which gave difficult identifiable problems in the beginning.

The model is running now and I can really appreciate its pragmatics and applications. It is very satisfactory that after 4 months of programming data for a model area as big as the Netherlands, but with a dataset so scarce, the model is finally up and running. Thank you to my supervisors Marta Faneca Sanchez, Gijs Janssen and Gu Oude Essink for guiding me in a very educative and exciting internship. I really enjoyed my stay at Deltares!

1. Overview model

The area of interest is established as the area south of the Ganges River, west of the Ganges estuary and east of the western land border of Bangladesh (figure 1.1 black border). A general head boundary[1] will be placed a certain distance from this area of interest to make sure it does not affect calculations in this area. The total model domain is therefore slightly larger than our area of interest (figure1.1). The total model domain covers an area of 274x317 = 86858 km^2.

CEGIS is the prime resource for data. This data often only focuses on our area of interest, thus the area towards the general head boundary is filled with other data sources. The resolution of the model is 1000m, which amounts to 274 columns and 317 rows in the model domain. The model units are meters, days, grams and litres. The density-dependent groundwater flow model SEAWAT in combination with the iMOD interface is used.
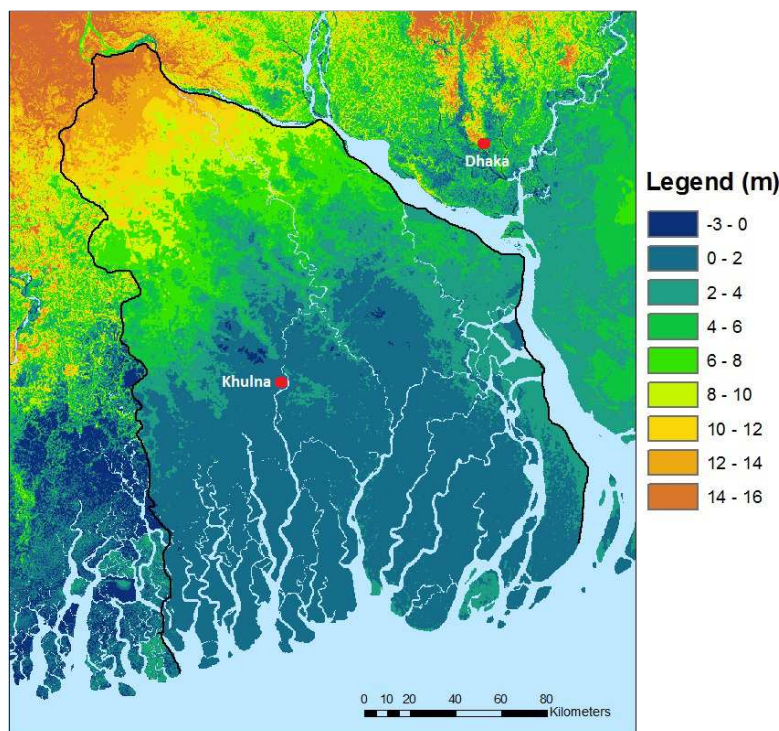
Figure 1.1: Illustration of total model domain and the area of interest (within black border). A general head boundary will be placed along all the borders of the model domain.

The model consists of 40 layers ranging in depth from 15m (top of the upper model layer) above msl (mean sea level) to 3000m below msl. The bottom of the model is a no flow boundary, which represents the low permeability Boka Bil formation (as in Michael and Voss, 2009b). Discretization of the model layers is shown in table 1.1 (appendix 4.1).

Thickness of layer (m)	Number of layers (-)
5	24
10	2
25	7
100	2
500	5

Table 1.1: Overview of the model layer discretization.

---

[1] A general head boundary is a boundary condition used to simulate head-dependent recharge or discharge across a groundwater system boundary.

Model stress periods

Since there are three distinct seasons in Bangladesh, the model simulates three stress periods: 1) a cold dry winter from November to February, 2) a humid hot summer from March to May and 3) a cool rainy monsoon season from June to October[23]. These three stress periods are only influencing the top system (precipitation, evaporation and rivers). Other data is divided on a wet/dry period (two stress period) basis. This means in the three stress period system, this data will have two stress periods of the same information (stress period November to February and stress period March to May). For convenience, these three stress periods are further referred to as stress period 1 for the November-February period, stress period 2 for the March-May period and stress period 3 for the June-October period.

Model boundary conditions

The IBOUND (active/inactive cells) is established such that model cells located below the surface elevation are active in every layer and model cells located above the surface elevation are inactive. The top of each layer describes the elevation of a layer. Thus for layer 1 all cells equal or higher than 15m are set active. This also applies for the bottom of the model. Every cell located above the model bottom (the Boka Bil formation; Michael and Voss, 2009b) is set active and below this elevation is set inactive in each layer. River cells are placed at the location of rivers at active cells for the layers 1-5 (figure 1.2 blue). From layer 6 (<-5m) onwards a general head boundary is placed (figure 1.2 red) to sustain sea salinity concentrations. Since the main flow direction is North-South (Michael and Voss, 2009b), there is also a general head boundary placed of one cell thickness at the northern border of the model domain (figure 1.2). The conductivity of these general head boundary cells is set at 1000m day^{-1}. Such a high conductivity virtually yields a constant head boundary. The concentration is set at 0.1g L^{-1} at the northern GHB and at 31g L^{-1} at the seaside GHB (section 2.3). The head at these boundary cells is set equal to the elevation in the North and bathymetry in the South. A no flow boundary condition is imposed on the Eastern and Western boundary of the model domain.
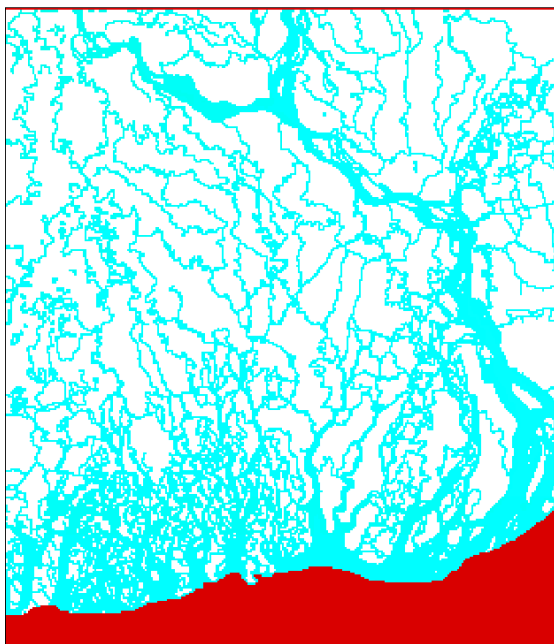
Figure 1.2: Illustration of the general head boundary and river boundary in the model domain.

2. Data processing

This section contains a description of: 1) the available data, 2) the discussion about which data to use and 3) the discussion about how to use the data in the model.

2.1 Digital elevation map (BAS and GHB)

Two digital elevation maps are used: 1) CEGIS DEM (300m), which covers the area of interest and 2) the DEM of the groundwater flow model of Michael and Voss (2009b) (MV DEM) (5000m). The digital elevation map of CEGIS is used because it corresponds best to expected elevation levels (sea level in the coastal zone) and has the highest available resolution (300m). Where there is absence of elevation data of CEGIS (northern and western area of our model domain), the MV DEM is implemented. This MV DEM is adapted in order to fit with the CEGIS DEM in the following way: the original resolution of 5000m is resampled to 1000m. The difference between the MV DEM and the CEGIS DEM is calculated and statistics show that the MV DEM is an average of 3.26m higher. The difference between the DEMS is contained in a map and wherever there is a no data value within the model domain, a value of 3.26 is assigned to such cells. This 'difference' map is subtracted from the resampled MV DEM. The result is a corrected MV DEM to fill in the missing parts in our model domain (figure 2.1). The digital elevation map will be used as a representation of the starting heads in the model.
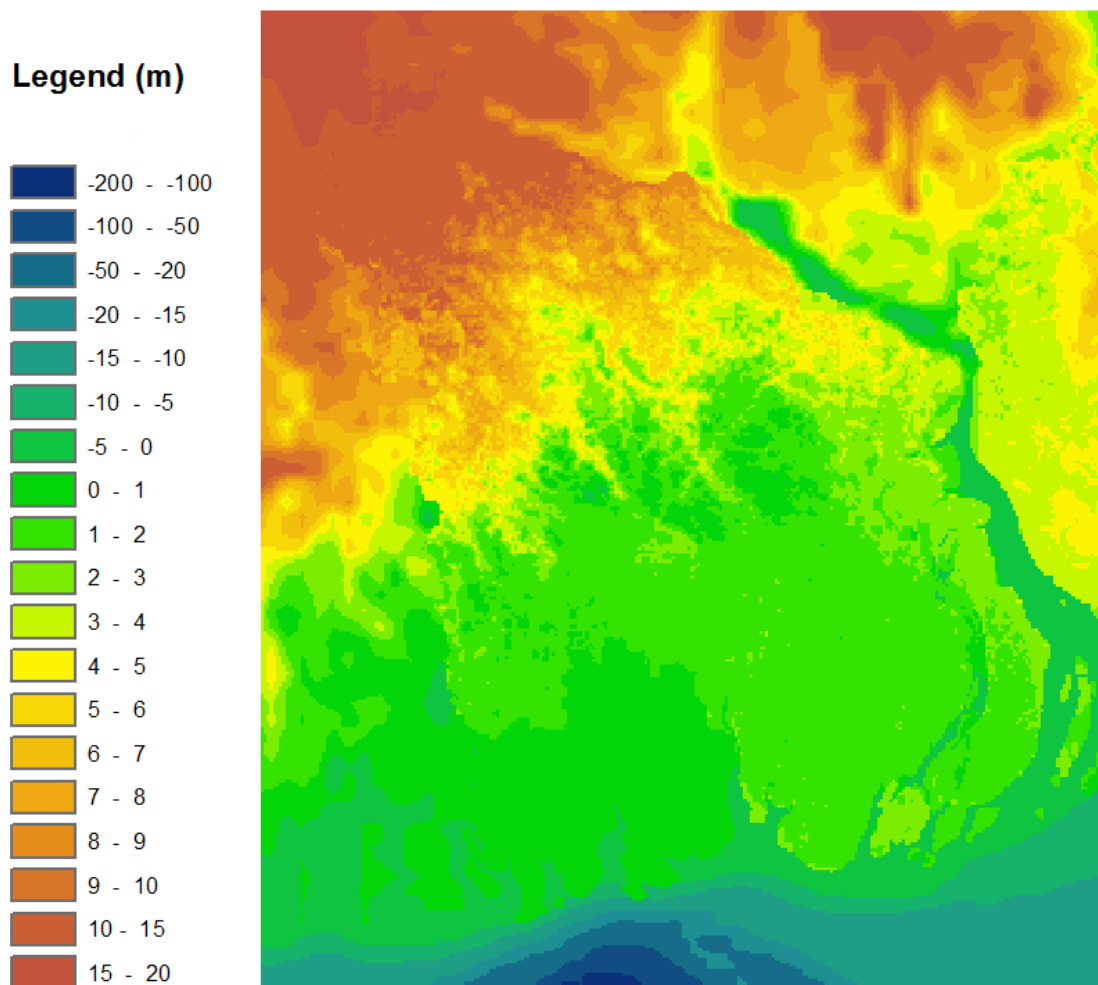
Figure 2.1: Compiled elevation map from CEGIS and the DEM from the model study of Michael and Voss (2009b).

2.2 Hydrogeology (BCF)

Borehole datasets of the lithology in our model area are available. Analyses of these datasets reveal a high degree of heterogeneity in the lithology as is supported by literature (detailed description of hydrogeological properties: Michael and Voss, 2009a). Stratigraphy of units is difficult to identify. Due to the lack of other complementary information in the borehole datasets, such as to which sequence the lithology belongs, the age etc., one method was to create a voxel model with an interpolation routine to fill in the 3D volume (Jan Gunnink TNO). This would result in a very heterogeneous hydrogeology due to the high variability in lithology in the boreholes. However, the voxel model would be inaccurate due to the often large distances between boreholes. The high degree of variability in lithology in a borehole has a different scale than the distances between which boreholes would be interpolated. Also, the 1000m resolution of the model and the thickness of the model layers would represent this heterogeneity, of which we know it exists, as one homogeneous bulk after averaging to define layer properties per layer and cell. Another problem of this heterogeneity is that it would result in a very odd distribution of fresh and salt water, which is not likely to be true, since the voxel interpolation gives a degree of heterogeneity, but not the actual lithology in an area. This fresh/salt distribution is important and the reason why a more layered stratigraphy in the model is highly desired.

To avoid these problems, an alternative approach was sought. Insights obtained from research about aquifer distribution, previous groundwater modelling studies in Bangladesh and available generalized geological cross-sections of the area resulted in the decision to use the hydrogeological cross-section of BGS and DPHE (2001) as a reference for lithology and aquifer distribution. Another reason to proceed this way is the knowledge that a PhD student from Holly Michael (Assistant Professor at the University of Delaware) is researching the geology in the Khulna area and has the goal to create a 3D geology set-up with better resources, time, and software. Ideally this 3D geology set-up could complement and improve our model in the future. This means that the borehole datasets are discarded in the build-up of the hydrogeology of the SWIBANGLA model.

The BCF file of the model of Michael and Voss (2009b) is also available; however they used a homogeneous anisotropic approach, because of the high degree of discontinuity in the geology and their large basin scale focus. This approach is not suitable for our model purpose, since our scale of interest is much smaller.

This section also describes the data information and processing of the borehole datasets before the decision to discard this data. This is done to show the total process of decision making in how to build up the hydrogeology of the SWIBANGLA model.

2.2.1   Borehole datasets

Available data are the borehole datasets of BWDB (delivered by CEGIS) and that of Holly Michael (source: DPHE). The borehole dataset of BWDB consists of 341 boreholes (figure 2.2) with a maximum depth of about 440m. The materials at those depths are described by several combinations of sub-materials: shale, concretion, peat, decomposed material, clay, mica, silt, very fine sand, fine sand, medium sand, coarse sand and gravel. These sub-materials are combined to one material and result in 290 unique material codes with about 65 combinations of percentages of amounts of sub-materials. For example, SLTVSDMIC701505, means 70% silt, 15% very fine sand and 5% mica.

The lithology dataset of Holly Michael consists of 396 boreholes with a maximum depth of 378m and with an interval of 3m (figure 2.2). It is described by six lithological units:

1. Clay
2. Silt/Silty clay/Sandy clay
3. Very fine sand/Fine sand
4. Medium sand
5. Coarse sand
6. Gravel
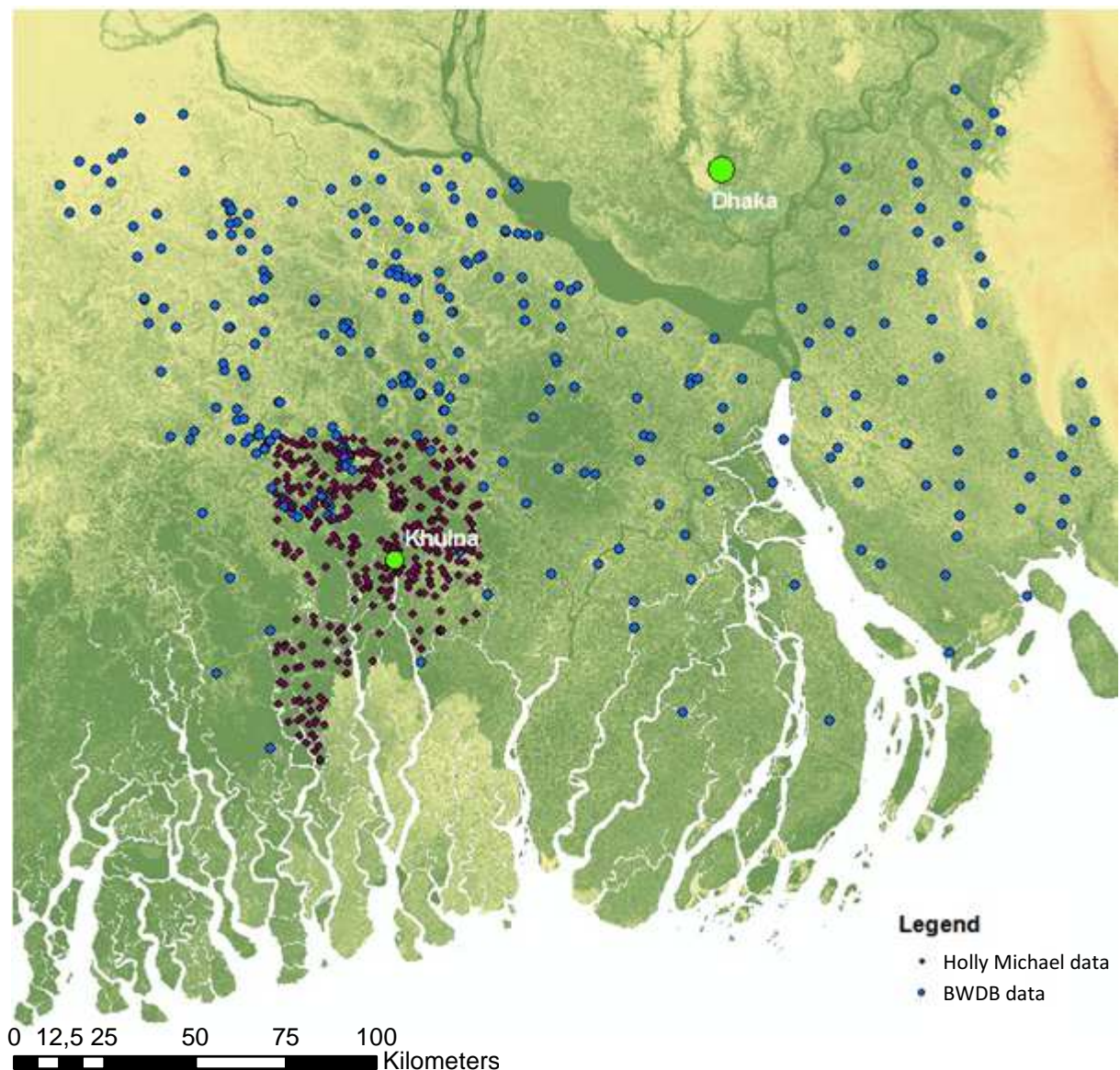
Figure 2.2: Locations of the boreholes of BWDB and Holly Michael in the area.

The dataset of Holly Michael already represents geology on a hydrological conductivity basis. Therefore it is convenient to subdivide the BWDB dataset over these classes.

It is not very clear where to put the sub-materials: shale, concretion, peat, decomposed material and mica of the BWDB dataset, because the division also depends on the combination of sub-materials

and the amounts of each sub-material in a material. Also, combinations such as CLYFSDVSDSLTMIC are present, which is a material consisting of clay, fine sand, very fine sand, silt and mica, and are difficult to classify as one unit. A solution to classify the BWDB data might be that of a combination of sub-materials only the dominant material is selected and is distributed by that characteristic over the classes of Holly Michael's dataset. 50% and higher of sub-material is defined as the dominant material and therefore describes the material. Then the example of SLTVSDMIC 701505 is dominantly silt and belongs to class 2 of Holly Michael's classification.

If a small sub-model (more local) is desired, the Khulna area would be suited, since all of Holly Michaels borehole data is clustered there, which would support a geologically more precise model.

A 3D representation of this borehole classification is shown in figure 2.3, which clearly shows the lack of stratigraphy. To reveal more stratigraphic units, the sand classes (very fine sand, medium sand and coarse sand) were added together. However, this did not increase the stratigraphy of the lithology. As already described, the decision was made not to proceed any further with the borehole datasets in the build-up the hydrogeology of the model.
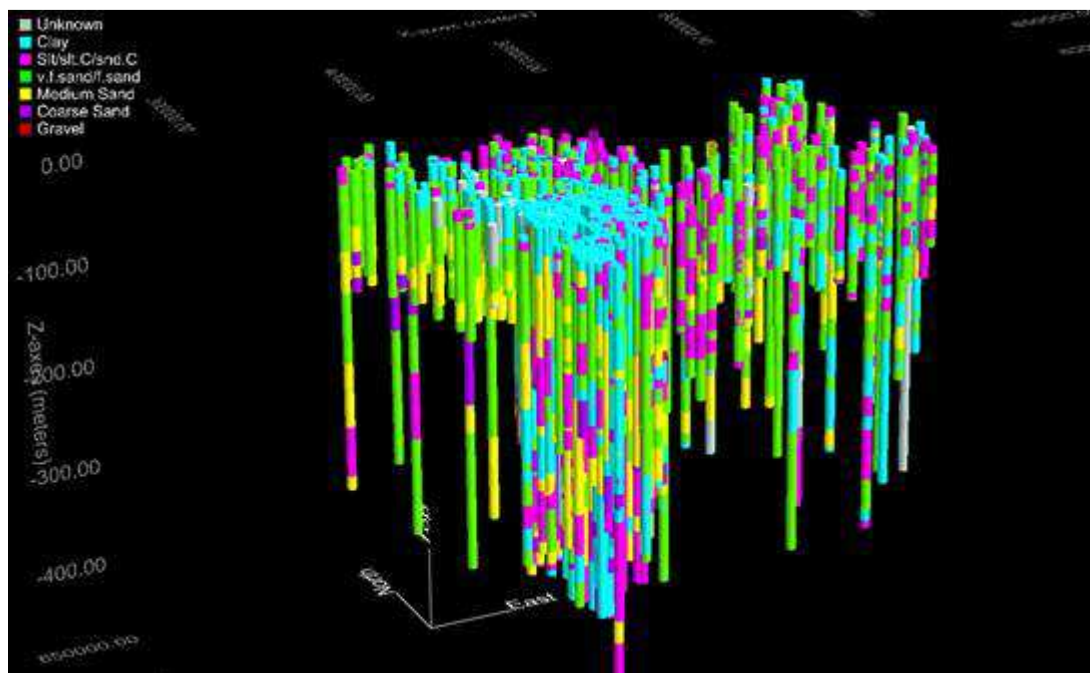
Figure 2.3: 3D representation of the borehole datasets of CEGIS and Holly Michael shown in iMOD.

2.2.2 Aquifer classification and groundwater modeling in Bangladesh

The first aquifer classification in Bangladesh was made by UNDP (1982). This classification consists of three aquifers up to a depth of 140 m: 1) upper or composite aquifer, 2) main aquifer and 3) deep aquifer. The model of UNDP (1982) only involved the upper 2 aquifers with a silty clay layer on top, but does not involve the deep aquifer. This system was updated by the Master Plan Organization (MPO, 1987: table 2.1) during the formation of the National Water Plan in 1985 on the basis of more than 17000 shallow bore logs. This dataset was combined with a limited number of deep oil and gas exploration well logs by Jones (1985) and resulted in an aquifer description containing two aquifer sequences, an upper and a lower sequence (the lower one was based on data of Jones, 1985). The upper aquifer system has a threefold sequence: an upper silty clay (2 to 100m thick) overlaying a fine

sand and silt aquifer known as the composite aquifer (3 to 60m thick); and the main aquifer composed of moderate to well sorted medium to coarse sands (30 to more than 100 m thick). The development of the upper aquifer sequence is limited by the poor storage properties of the overlying silts and clay (MPO, 1987). Aquifer test data prove that the whole of the upper aquifer sequence behaves as a single multiple aquifer system in which all the units are hydraulically connected (MPO, 1987). The majority of the main aquifer can be classified as unconfined or semi-confined.The groundwater in the deeper aquifers is recharged from outside the Bangladesh plains on its eastern unconfined outcrop in the Tripura and Sylhet hills (Jones, P.H., op. cit. from MPO 1987; Hoque and Burgess, 2012; Majumder et al., 2011).The deep aquifer of the UNDP (1982) classification has been included into the lower aquifer sequence. This lower aquifer sequence is further divided into five aquifers separated by clay aquitards. However, the interpretation of the limited number of data in the lower aquifer sequence in terms of hydrogeology is highly speculative. The MPO report (1987) states that there is no adequate data of the lower aquifer sequence and is not further discussed in terms of aquifer properties.

Aquifer sequence	Sub-units	Thickness (m)	Comments
Upper aquifer sequence	Silty Clay	0 to 120	Based on 17000 well logs
	Composite Aquifer	3 to 60	
	Main Aquifer	30 to 60	
Lower aquifer sequence	Clay Aquitard	20 to 80	Hypothetical, based on 36 well logs and 20 geo-electrical logs (Jones 1985). Hydrogeological interpretation speculative.
	Aquifer No. 2	60 to 120	
	Clay Aquitard	0 to 170	
	Aquifer No. 3	140 to 180	
	Clay Aquitard	110 to 140	
	Aquifer No. 4	100 to 170	
	Clay Aquitard	100 to 160	
	Aquifer No. 5	80 to 150	
	Clay Aquitard	30 to 50	
	Aquifer No. 6	110 to 190	

Table 2.1: Aquifer classification by MPO (1987).

EPC (Engineering and Planning Consultants) and MMP (M. MacDonald and Partners) created a more flexible four-layer model of Bangladesh in 1991 building further on the aquifer distribution of UNDP (1982) (BGS and DPHE, 2001) (table 2.2). The subdivision of Bangladesh aquifers into three or four layers has proved adequate for assessing the water balance for aquifers in much of the country (BGS and DPHE, 2001). However, they do not include modeling of the deeper aquifers.

Layer Description	Layer Geology	Thickness (m)
1 Upper Aquitard	Upper alluvial sequence; micaceous silts and fine sands	5-25
2 Upper Shallow Aquifer	Upper alluvial sequence; medium to fine sands	20-40
3 Lower Aquitard	Lower alluvial sequence; clays and very fine sands	2-10
4 Lower Shallow Aquifer	Lower alluvial sequence; medium to coarse sands and gravels	25-60

Table 2.2: The four-layer aquifer model of Bangladesh (after EPC/MMP, 1991). The three-layer model of UNDP (1982) discards the lower aquitard layer in the model.

The British Geological Survey (BGS) and the Department of Public Health Engineering (DPHE) constructed a geological cross-section of the Mid- to Upper Quaternary sediments North to South through Central Bangladesh (figure 2.4). In the coastal zone several fining upward sequences are present as a result from the deposition patterns during glacial/interglacial cycles. This alternation of sandstones and silts contains saline water above fresh water in a series of discrete aquifers in the coastal zone, but unite to form a single body of fresh water past the limit of salt water intrusion (BGS and DPHE, 2001). This hydrogeological cross-section is chosen to represent the aquifer distribution in the SWIBANGLA model. Table 2.3 shows an overview of the mentioned aquifer classifications.
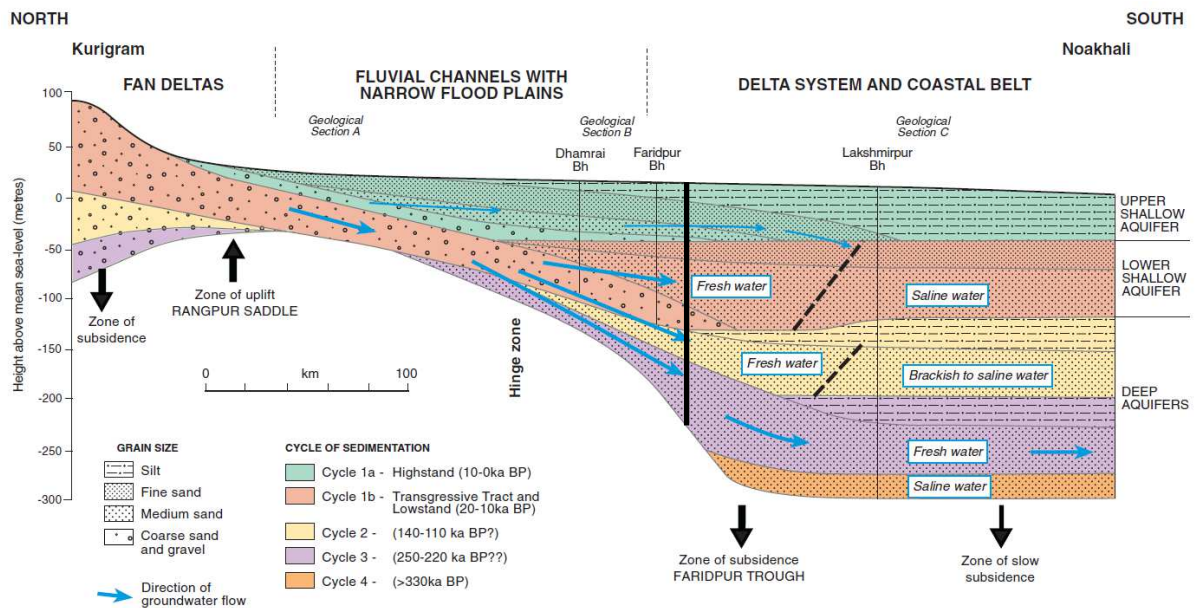
Figure 2.4: Hydrogeological cross-section from north to south across Bangladesh. Particularly shown are the geological structure and groundwater flow patterns within Mid- to Upper Quaternary sediments. The thick black line shows the location of the Northern border of the SWIBANGLA model domain in this cross-section (BGS and DPHE, 2001).

UNDP (1982)	EPC and MMP (1991)	MPO (1987)		BGS and DPHE (2001)
Upper aquifer	Upper aquitard	Upper aquifer sequence	Silty clay layer	Upper shallow aquifer
	Upper shallow aquifer		Composite aquifer	
Main aquifer	Lower Aquitard		Main aquifer	Lower shallow aquifer
	Lower shallow aquifer			
Deep aquifer *(classified, not in model)*	Deep aquifer *(classified, not in model)*	Lower aquifer sequence	Alternating aquifers and clay aquitards	Deep aquifers

Table 2.3: Overview aquifer representations. The models of UNDP (1982) and EPC and MMP (1991) do not involve the deep aquifer (BGS and DPHE, 2001).

2.2.3 Model bottom: deep aquifer separation by clay layers

There is mention of separation of the upper and deeper aquifers by a clay layer. From the literature it is known that clay layers do occur and are defined as the separation between the upper and deeper aquifers (Banglapedia[4]; MPO, 1987; Majumder et al., 2011; McArthur et al., 2004; Klump et al., 2006). DPHE/UNICEF/WB define deep aquifers not by a certain depth, but also by the presence

[4] http://www.bpedia.org/A_0280.php

of an aquitard or aquiclude separating the shallow and deep aquifers (DPHE/Gob/APSU/JICA, 2006). Morton and Khan (1979) report that the deep aquifer is overlain and protected from vertical intrusion of saline water by a 65 to 165m thick clay layer. The hydrogeological cross-section of BGS and DPHE (2001) also shows some low permeability layers between the aquifers. Ideally this more shallow clay layer could be used to define the model bottom, which is normally a no flow boundary. However, several cross-sections, literature and the borehole data of Holly Michael and BWDB do not show a closed layer. According to Michael and Voss (2009a) the basin consists of a stratified, heterogeneous sequence of sediments with aquitards that may separate aquifers locally, but evidence does not support existence of a regional confining unit. The silty-clay layers are of limited lateral extent within the aquifer system. Together these layers still impose a hydraulic anisotropy on the aquifer which can strongly control the groundwater flow system within the basin (Michael and Voss, 2009a; Hoque, 2010; Mukherjee et al., 2007). Michael and Voss (2009b) searched for an impervious base in geology as to define the model bottom in their Bengal Basin model. They defined the low permeability Boka Bil formation as the model bottom where it exists, or the Precambrian basement is chosen where the Boka Bill formation is absent or not identified. This no flow boundary is also used in the SWIBANGLA model.

2.2.4   Model building of the hydrogeology

The North-South hydrogeological cross-section (BGS and DPHE, 2001: figure 2.4) is chosen to represent the aquifer distribution in the model. This cross-section ranges from Kurigram in the North to Noakhali in the South (figure 2.5). The 218 kilometer length part is taken for our model area and interpolated over the models North-South length. This section is marked by the vertical black line in the hydrogeological cross-section (figure 2.4). Figure 2.6 shows the representation of this cross-section in the SWIBANGLA model area (see Appendix 4.2 for elevation information).
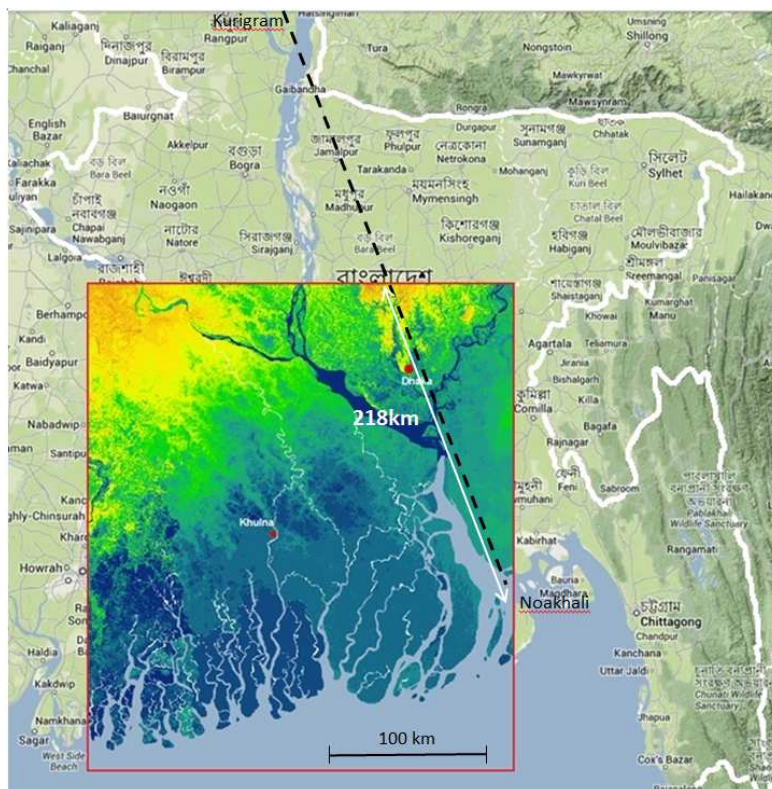
Figure 2.5: The position of the hydrogeological cross-section of BGS and DPHE (2001) in the SWIBANGLA model domain.
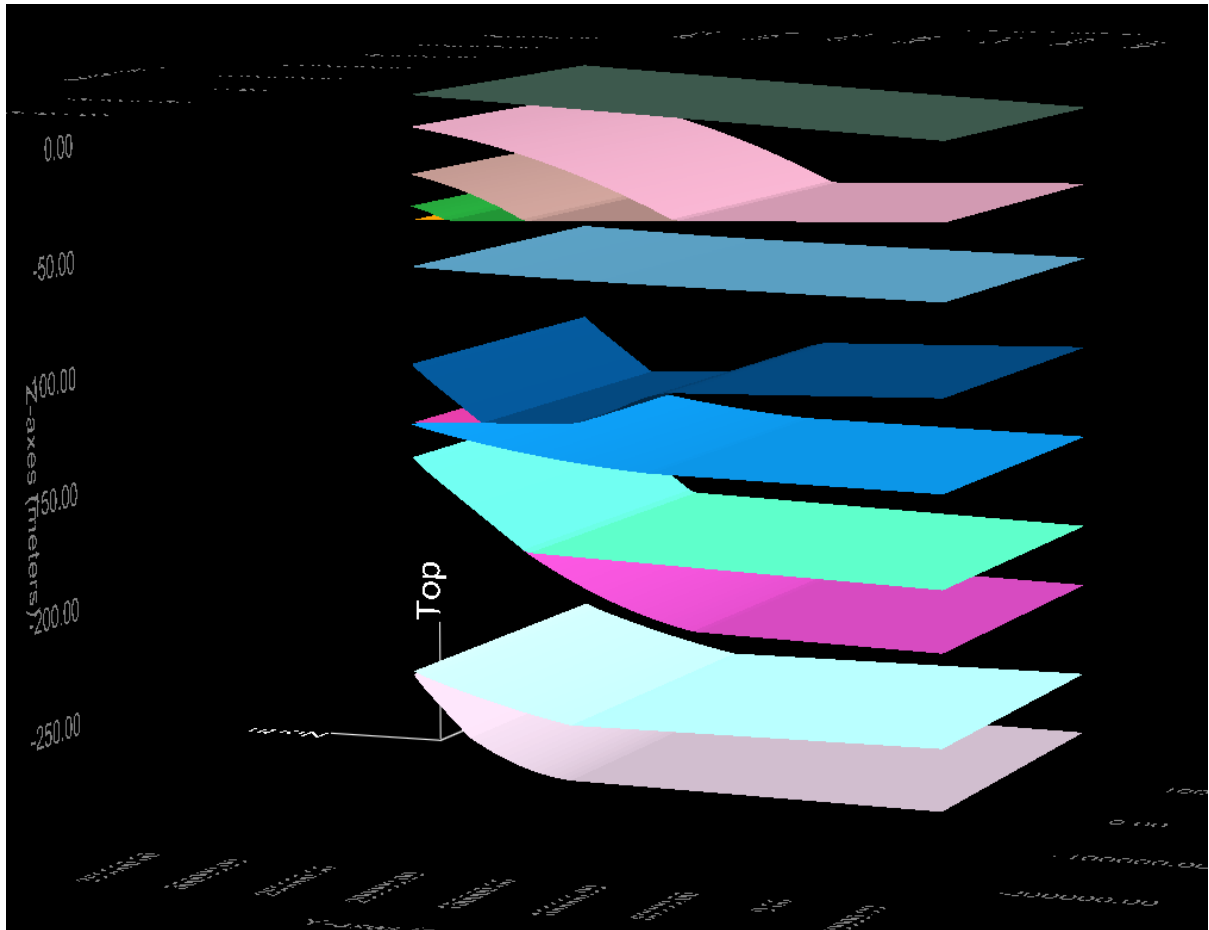
Figure 2.6: BGS and DPHE (2001) 3D cross-section representation of the SWIBANGLA model shown in iMOD. The layer planes mark transitions from one grain size to another (figure 2.4 appendix 4.2).

The Boka Bil formation, which represents the bottom clay layer in the model study of Michael and Voss (2009b), is extracted from the discretization file (or: the "DIS Package") of their Bengal Basin model and shown in figure 2.7.
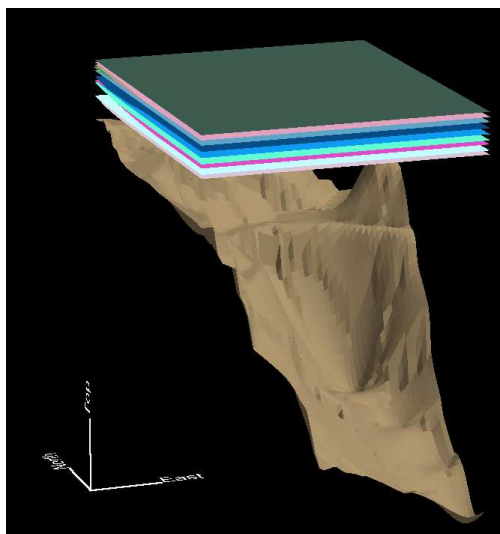
Figure 2.7: Boka Bil impervious bottom shown in iMOD. Deepest point is around 3000 m. The upper layer planes illustrate the 3D cross-section representation of BGS and DPHE (2001) in the SWIBANGLA model (figure 2.6).

2.2.5 Hydrogeological properties

The cross-section of BGS and DPHE (figure 4.2) divides the system into four lithological classes: silt, fine sand, medium sand and coarse sand/gravel. This paragraph explains the parameterization of these four lithology classes.

Table 2.4 shows the different permeabilities (m day^{-1}) for different sandy lithologies (red-brown and grey sediments) as described in Rahman and Ravenscroft (2003).

Lithology	Permeability (m day^{-1})		
	Brown	**Grey**	**Dhamrai Fm**
Fine sand/silt	8	16	6
Fine sand	13	***26***	12
Fine/medium sand	17	34	21
Medium/fine sand	21	42	37
Medium sand	25	***50***	53
Medium/coarse sand	34	68	60
Coarse/medium sand	38	76	70
Coarse sand	46	92	-
Coarse sand/gravel	42	***84***	70
Gravel/coarse/medium sand	25	50	35

Table 2.4: Correlation of lithology and permeability (MMI/HTS, 1992; Davies and Herbert, 1990 inRahman and Ravenscroft, 2003). The red highlighted values are used in the SWIBANGLA model.

The aquifers in the model area mainly consist of grey sediment rather than red-brown sediment (table 2.5). The red-brown sediments are less permeable due to weathering and the formation of iron-oxide cements (BGS and DPHE, 2001). Therefore, permeability values of the grey sediments in table 2.4 are used in the SWIBANGLA model.

| This study	UNDP, 1982	Fluvial area	Delta area
Upper shallow aquifer	Composite aquifer	Grey highstand braided floodplain aquifer (U Dhamrai Fm)	Grey highstand floodplain aquifer of dendritic distributary system
Lower shallow aquifer	Main aquifer	Grey coarse grained transgressive tract/lowstand aquifer in incised channels (L Dhamrai Fm)	Grey transgressive tract/lowstand aquifer within incised channels
Deep aquifers	Deep aquifer	Red-brown Dupi Tila of the Chandina area, and Barind and Madhupur Tracts.	Grey sub-150 m deep aquifers composed of cyclic, vertically stacked aquifers in subsiding delta

Table 2.5: Main aquifer divisions within the fluvial and deltaic areas of Bangladesh (BGS and DPHE, 2001).

The upper silt layer of the hydrogeological cross-section of BGS and DPHE (2001) is described in literature as the upper silty clay layer (MPO, 1987; Rahman and Ravenscroft, 2003). Vertical hydraulic conductivities of different soil textures including this upper silty clay layer can be derived from table 2.6. The vertical conductivity value of 5mm day^{-1} is taken to represent this upper silty clay layer, which is the minimum bound of permeability of the dry and wet season. This value is also assigned to the other silt layers in the hydrogeological cross-section of BGS and DPHE (2001). The vertical hydraulic conductivity is set as one tenth of the horizontal hydraulic conductivity. Thus the horizontal conductivity for the silt layers in the hydrogeological cross-section of BGS and DPHE (2001) is set at 50mm day^{-1}.

Soil texture	Vertical hydraulic conductivity (mm day^{-1})			
	Wet Lands		Dry Lands	
	Min.	Max.	Min.	Max.
Fine sandy loam	25	40	25	20
Silty loam	15	24	10	80
Loam	25	40	15	120
Silty clayey loam	15	24	15	120
Clay loam	10	16	5	120
Silty clay	5	8	5	40
Clay	5	8	5	40
Sandy clay loam	15	24	15	120

Table 2.6: Top soil vertical permeabilities (MPO 1987 in Rahman and Ravenscroft, 2003). Wet lands conductivities refer to the wet season and dry land conductivities to the dry season.

Table 2.7 shows the horizontal hydraulic conductivity values that are used to construct the conductivity ascii's for the model for the upper 300m (hydrogeological cross-section of BGS and DPHE, 2001). Information about the lithology below this depth is not present/unavailable.

Lithology	Horizontal hydraulic conductivity (m day^{-1})	Vertical hydraulic conductivity (m day^{-1})
Silty	0.05	0.005
Fine sand	26	2.6
Medium sand	50	5.0
Coarse sand/gravel	84	8.4

Table 2.7: Horizontal conductivity values used in the SWIBANGLA model.

2.2.6 Hydrogeological properties below the depth of the cross-section of BGS and DPHE

The MPO report (1987) mentions that at depths in excess of 300 m there is very few data. Below the Pleistocene sediments there is mention of the Surma formation, which is of Miocene age, but there is no description of the lithology. At this point there are 7 layers (appendix 4.1) in the model of which the hydrogeological properties are unknown.

The hydraulic conductivity values from the study of Michael and Voss (2009b) are taken for the deeper layers. This is an average of the southern delta conductivity and the central floodplain conductivity, which is 17m day^{-1}. The vertical conductivity below 300m depth is set as a tenth of this horizontal hydraulic conductivity.

2.3 Groundwater salinity (BTN)

Groundwater salinity data is delivered by CEGIS and consists of three sections: 1) groundwater salinity (-), 2) groundwater quality (DPHE) and 3) groundwater quality (BWDB). The groundwater salinity file contains salinity data at only 7 locations for about 1992 till 2003. However, the locations of these measurements are not known and therefore this data is discarded (no response from CEGIS). The groundwater quality file of DPHE contains electrical conductivity measurements in $\mu S \; cm^{-1}$ for 136 locations (figure 2.8) with a maximum well depth of 390.03m for the years 1960-1992[5]. The measurement interval is a few times a month (alternates with sometimes 6 times a month and sometimes zero). Every measurement location has only one measurement depth. To attain an EC-depth profile more measurements at one location are needed and therefore the fact that these wells are located in clusters is used. All wells in every cluster are assumed to have the same location and EC-depth profiles are established. The groundwater quality file of BWDB does only incorporate EC measurements at a few locations of which even fewer are close enough to incorporate in a DPHE cluster. This data is therefore also discarded. The established EC-depth profiles based on the DPHE data do not show any sign of a fresh-salt interface. In the whole model domain the values are approximately the same (appendix 4.3). Also EC-values close to the coast are considerably low. For example locations 02-002 and 02-008 (figure 2.8) have a maximum EC of 966 and 923 $\mu S \; cm^{-1}$ respectively.
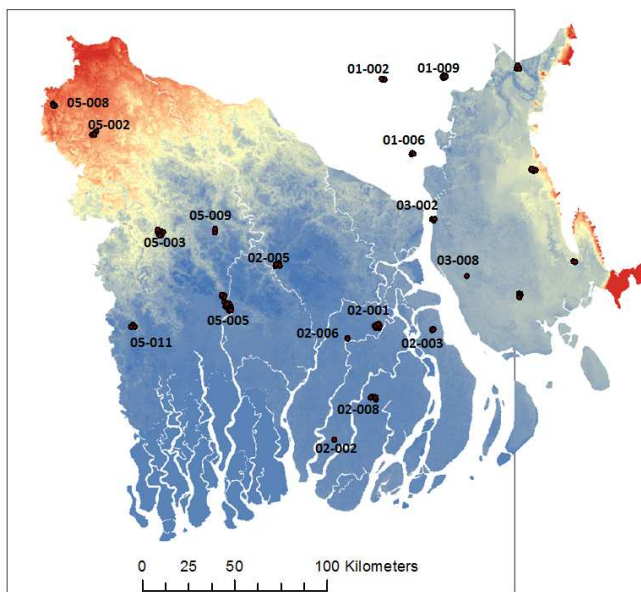
Figure 2.8: Locations of the 136 groundwater quality wells in the area (DPHE). These wells are distributed in clusters. The associated label is to define the location of a cluster.

Since the previously described data does not suffice to establish salinity rasters per layer, the hydrogeological profile of BGS and DPHE (2001) is used. This profile also shows the distance and depths of salinity intrusion (figure 2.9)[6]. The salinity front in the upper aquifer is located at 187km (South border of model domain as a reference: 0km) at 40m below msl and extends to 133m below msl at 234km. The salinity front in the second aquifer is located at 182km with a depth of 153m

---

[5] *Note: the unit associated with the EC measurements was not clear. The unit of $\mu S \; cm^{-1}$ was defined based on the magnitude of the EC values.*
[6] The data on which this salinity front profile is based is not known.

below msl and extends to 194m below msl at 218km. This salinity front roughly corresponds to the salinity front shown in figure 2.10 (BADC, 2011).
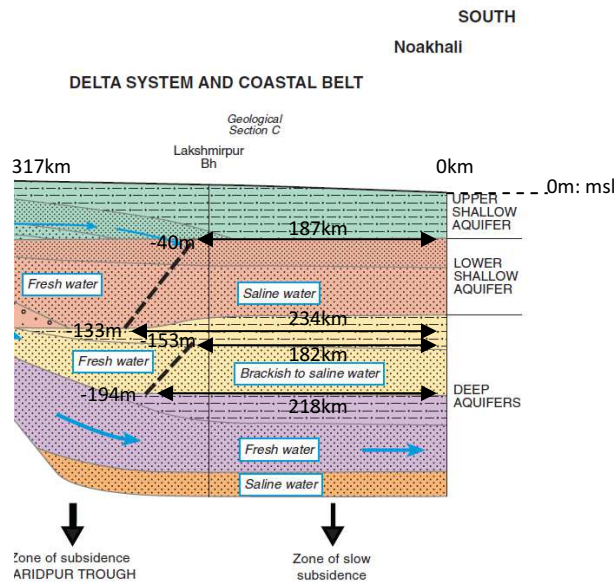
Figure 2.9: Salinity front shown in the hydrogeological cross-section of BGS and DPHE (2001).
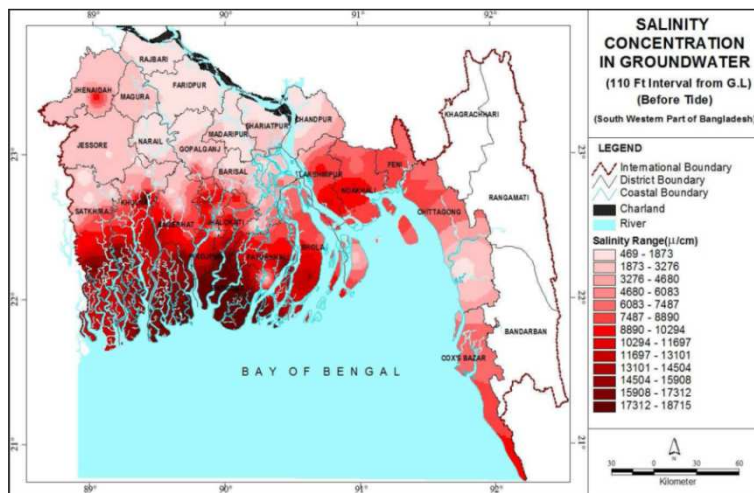
Figure 2.10: EC map at 35 meters depth established by the Bangladesh Agricultural Development Corporation (BADC, 2011) based on 100 observation wells with salinity measurements at a 10ft interval.

When the salinity front as established from the BGS and DPHE cross-section runs through a cell, the concentration of such model cell is a combination of the fraction of saline water and the fraction of fresh water. Thus if the salinity front very conveniently runs through a cell and splitting it in half, a combination of 50% fresh water and 50% saline water will be used as a concentration. The salinity of the water will be put in the model as Total Dissolved Solids (TDS). The salinity of saline water is set at 31g L^{-1} (National Institute of Oceanography[7]; Benshila et al., 2014) and that of fresh water at 0.1g L^{-1}. The salinity of brackish to saline water (figure 2.9) is set at 16.5g L^{-1}. The salinity below 300m depth (maximum extent of the hydrogeological cross-section of BGS and DPHE, 2001) is not known and is set at the same salinity present at 300m depth (31g L^{-1}) to avoid unwanted large vertical fluxes due to density differences.

---

[7] http://www.nio.org/index/option/com_nomenu/task/show/tid/2/id/140

2.4 Abstraction rates (WEL)

2.4.1 Domestic and industrial abstraction

The abstraction rates of domestic and industrial water use are based on population amounts, which is in accordance with the method used in the groundwater model of Bangladesh of Michael and Voss (2009b). The total (domestic + industrial) demand in 2003 was estimated to be approximately 50 L day^{-1} per capita (WARPO, 2000). Population numbers of the 2011 census of Bangladesh[8] and India[9] are used with an annual growth rate of 2.09% for Bangladesh (CIA, 2006) and an annual growth rate of 1.58% for India[10].

The population amounts are given per upazila (sub-district). In order to define an abstraction per model cell, the geographical surface area for every upazila is calculated in ArcGIS. The population numbers of 2011 are multiplied by the growth rate and the water use (0.05 m^3 day^{-1}), and divided by the surface area (km^2) of the upazila. The resulting unit of abstraction is m^3 day^{-1} km^{-2}. This method assumes a spatially homogeneous distribution of both the population and the groundwater abstraction rates in each upazila. Figure 2.11 shows the abstraction map of domestic and industrial use. It is assumed that domestic and industrial abstraction is constant throughout the year, which means the same rates are used in each stress period.

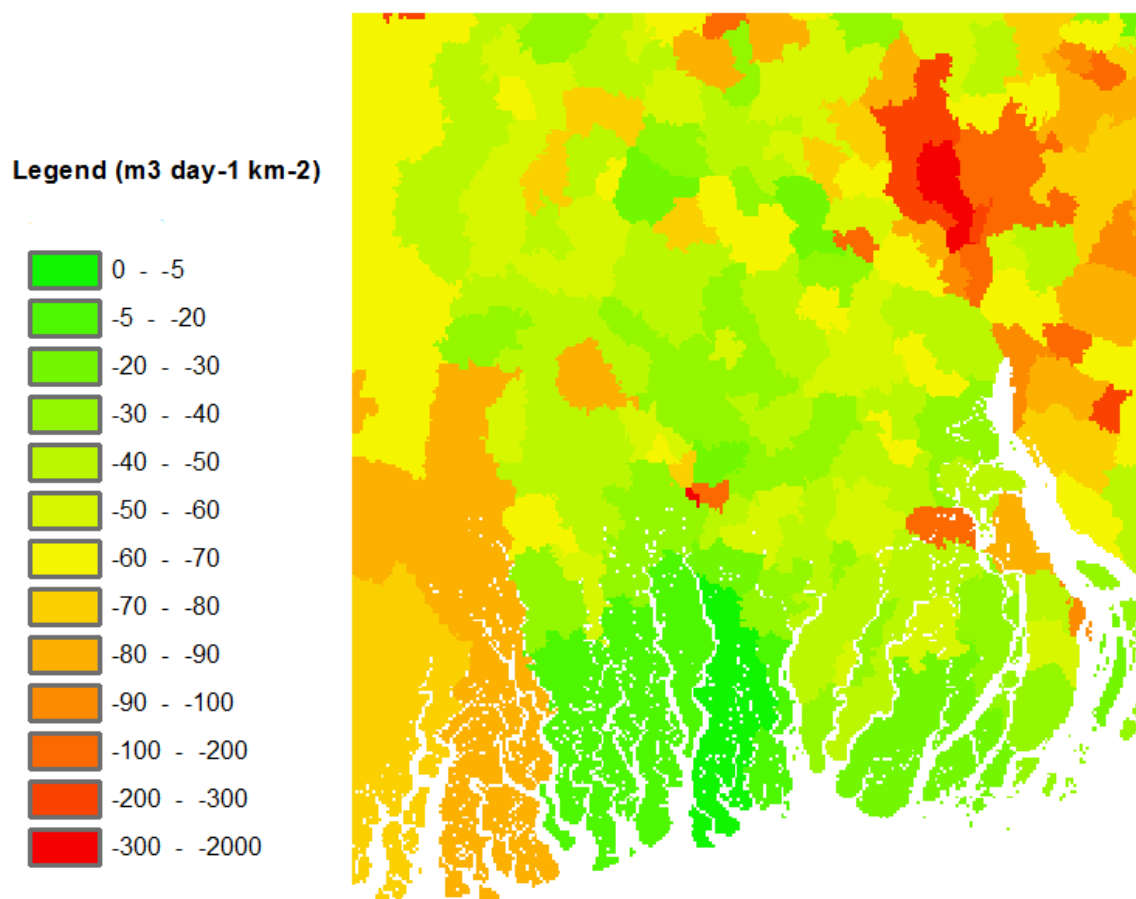Figure 2.11: Domestic + industrial abstraction per model cell (km^2) in m^3 day^{-1}.

---

[8] http://www.geohive.com/cntry/bangladesh.aspx
[9] http://www.census2011.co.in/district.php
[10] http://www.indiaonlinepages.com/population/india-current-population.html

2.4.2 Abstraction for irrigation

Irrigation magnitude in Bangladesh is related to the seasons (dry and monsoon season). Table 2.8 contains information about the distribution of abstracted irrigation water between seasons. The Kharif and Rabi season represent harvest seasons. In the Rabi season crops are sown in winter and harvested in spring (November to May). The Kharif season refers to crops that are sown in spring and harvested in autumn (June to October).

Irrigation technology	Rabi Season				Kharif season		
	Boro	Wheat	Others	Total	Aman	Others	Total
All STW	1,688,387	291,113	179,241	2,158,741	96,403	96,403	125,923
Force mode tube	824	29	64	917	11	11	17
DTW	416,115	33,846	24,561	474,522	29,290	29,290	32,059
Low lift pump	533,138	13,713	23,471	570,322	5,182	5182	5,990
Non-mechanised	21,387	6,584	10,370	38,341	728	728	728
Traditional	142,095	12,261	31,210	185,566	25,393	25,393	25,393
Total	2,801,946	357,545	268,918	3,428,409	157,007	157,007	190,110
canal irrigation				219,466			156,158
Grand total							3,994,143

Table 2.8: Number of wells per different pumping method and season[11] (1997).

Abstraction rates for irrigation use are divided over the wet (Kharif) and the dry (Rabi) season by the fraction between the seasons extracted from table 2.8, which is on average 0.05 and 0.95 respectively.

The irrigation data delivered by CEGIS contains the irrigated area in hectares for several types of pumping techniques (2006 report): 1) deep tube wells, 2) shallow tube wells, 3) low lift pump, 4) irrigation by manual, traditional method, artesian well and 5) irrigation by gravity flow. This data is present on a district level. The upazila level irrigation does not contain information about the method used, which is considered important due to the differences in depth of abstraction per method. Only the deep tube well (DTW) and the shallow tube well (STW) method affect groundwater flow. The other methods are related to surface water abstraction and are not considered in the model.

The abstraction rate is compiled by multiplying the irrigated area per district by an estimated 1.0m (Harvey et al., 2006) and dividing this value by the total surface area (km^2) of each district. This distribution method assumes a homogeneous distribution of irrigated surface area on the total surface area of a district. These values are divided over the stress periods on a 0.05-0.95 (wet and dry season respectively) basis. Also, because the delivered data is a one-year overview, the values are recalculated to abstraction per day according to the length of the two stress periods used, which is 212.25 days and 153 days for the wet and dry period respectively. This results in an abstraction rate (m^3) per cell (km^2) per day.

A part of the model domain is located over the border in India. Data on a DTW/STW basis is unavailable, thus a total amount of surface area irrigated per district is used[12][13][14][15][16].

---

[11] http://www.banglapedia.org/HT/I_0095.HTM

[12] http://agricoop.nic.in/Agriculture%20contingency%20Plan/West%20Bengal/WestBengal%207-Hooghly-31.12.2011.pdf

[13] http://agricoop.nic.in/Agriculture%20contingency%20Plan/West%20Bengal/WestBengal%2013-North%2024%20Parganas-31-12-2011.pdf

Figure 2.12 shows the rate of abstraction in the dry (stress period 1 and 2) and the wet season (stress period 3) for the model area. Shallow tube wells are more generally used over deep tube wells for irrigation purposes. The use of tube well irrigation is more excessive in the northern part of the model area compared to the southern part, which is likely to be the consequence of salinity intrusion in the coastal parts. Analysis of the irrigation data indeed shows that the majority of surface water irrigation techniques are located in the coastal zone (figure 2.13).
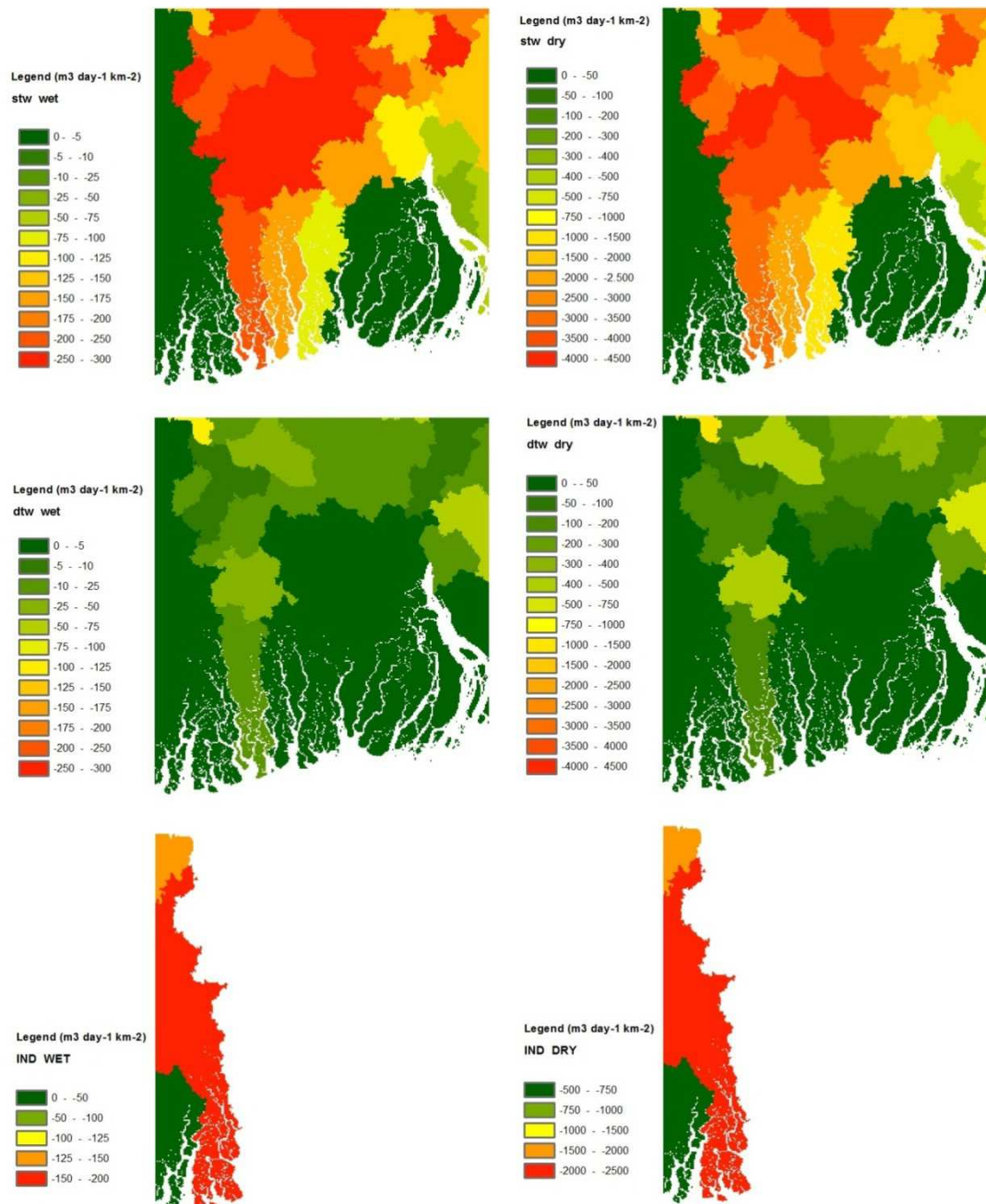
Figure 2.12: Abstraction rates in m^3 day^{-1} km^{-2} for deep tube wells (upper figures), shallow tube wells (middle figures) and India (lower figures) in the wet (left figure) and dry (right figure) season.

[14] http://agricoop.nic.in/Agriculture%20contingency%20Plan/West%20Bengal/WestBengal%2017-South%2024%20parganas-31.12.2011.pdf
[15] http://nadia.nic.in/Agriculture/agriculture.html
[16] http://agricoop.nic.in/Agriculture%20contingency%20Plan/West%20Bengal/WestBengal%2011-Murshidabad-31.12.2011.pdf

Figure 2.13: Fraction of the irrigated area by surface water methods of the total irrigated area in a district. Such data of the western part in our model (India) is not available.

2.4.3 Depth of abstraction

So far an abstraction rate per model cell (1 km^2) per day for domestic and irrigation purposes has been established. However, depths need to be assigned to the a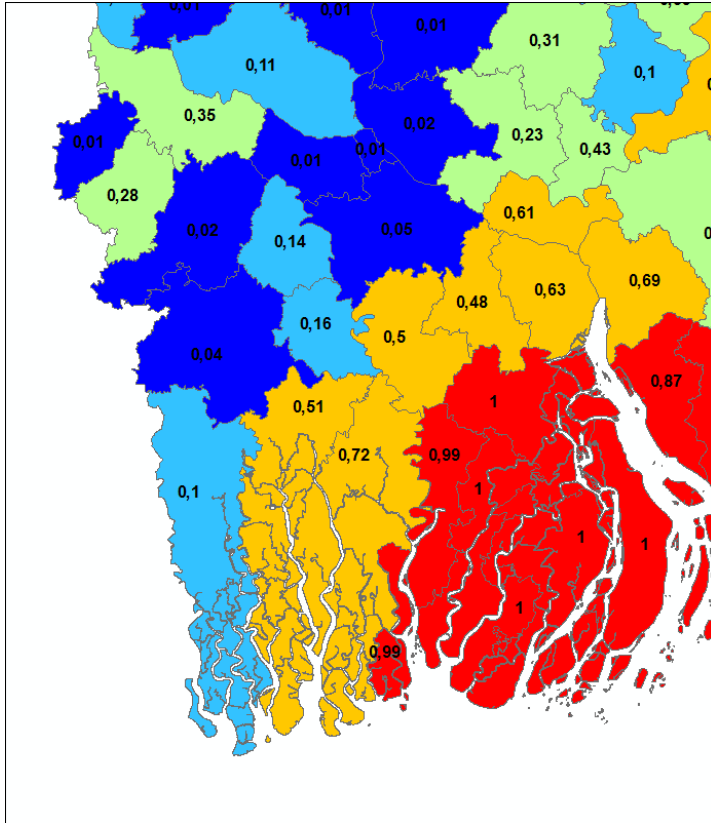bstraction rates, to be able to allocate them to model cells. It is estimated that 6-11 million tube wells are present in Bangladesh, the vast majority being private wells with a depth between 10 and 60m (BGS and DPHE, 2001). Irrigation wells typically tap deeper aquifers in the region of 70-100m depth (BGS and DPHE, 2001). Deep tube wells have been installed in the Southern coastal area to avoid high salinity at shallower levels (BGS and DPHE, 2001).

Abstraction for irrigation purposes was delivered on a STW and DTW basis. Information of CEGIS about the different irrigation techniques shows a definition of DTW depths for irrigation of 60-90m. STW irrigation depths from this same source of information are defined to have a depth less than 30m. In the Bengal basin model of Michael and Voss (2009b) a depth of 50-100m is used for abstraction by irrigation. Mondal and Saleh (2003) give a description of irrigation DTW being on average 100m deep and irrigation STW 40-60m. Based on such literature a depth of 10-60m depth is chosen for the STW and 60-100m for DTW irrigation. The abstraction rates (STW or DTW) are divided uniformly over the layers covering these depths. For example, a DTW abstraction rate is divided by 8 (layers present in the range of 60-100m with a 5m interval) and from each such layer at the location of the DTW this rate is abstracted. Since such data is absent for India, abstraction is equally divided over the total STW/DTW depth range, which is 10-100m.

Abstraction depths for domestic and industrial purposes are derived from data of DPHE[17]. This data is gathered as a number of documented abstraction wells per district and only focuses on the area of interest. Some of the districts contain over 200 documented wells, while others contain only 2 documented wells. Figure 2.14 also shows of which districts such data is present. The domestic abstraction in the Bengal Basin model of Michael and Voss (2009b) is set at a depth of 10-50m.
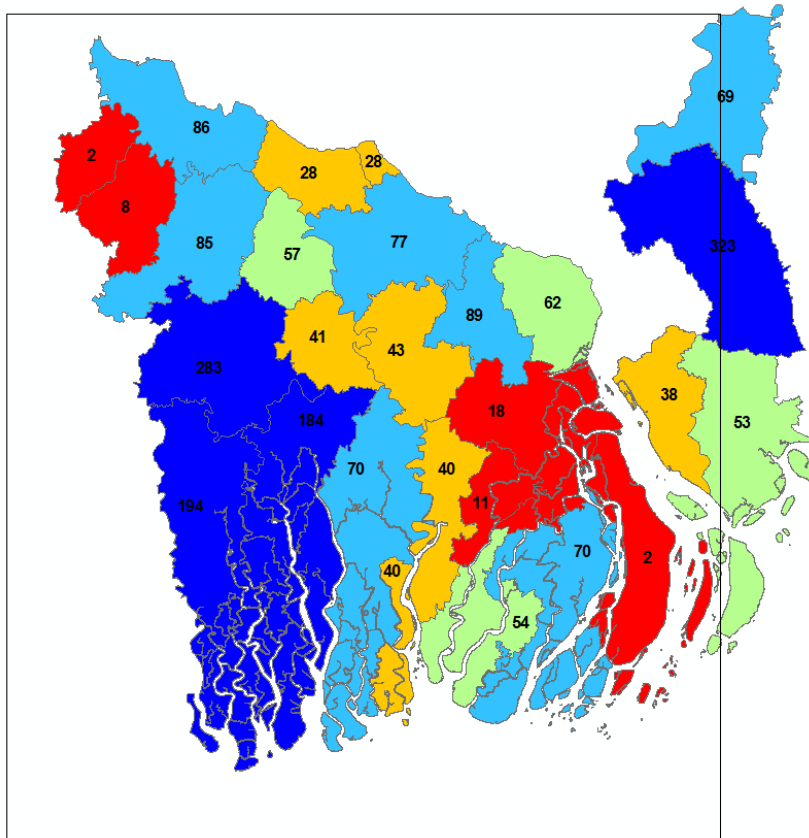

Figure 2.14: Overview of the number of point (well) data in each district on which domestic abstraction depths are defined, Black border indicates the model domain.

The domestic abstraction rate depth is defined as the abstraction between the minimum and maximum depth of wells in a district (figure 2.15). Thus, the layers between these depths are all equally affected by abstraction. In order to make sure that the minimum and maximum depth identified in a district are not outliers in the distribution of the well depths, the median and average depth of each district are compared. The closer together, the better distribution the well depth data has. Figure 2.16 shows that the well depth data in each district has a good distribution. This means that the associated minimum and maximum depths of each district are no outliers in their datasets. Abstraction depths of districts absent of such data and the part of India, are derived from the average minimum and maximum depth of the districts that do contain data. This means that domestic abstraction in these parts of the model domain occurs between 135m and 300m depth.

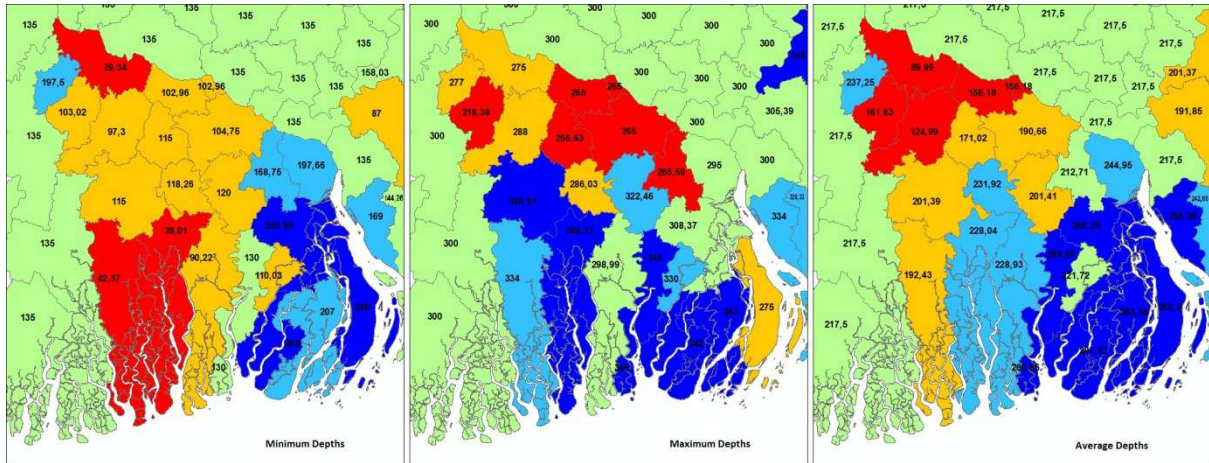[17] http://dphe.gov.bd/aquifer/index.php

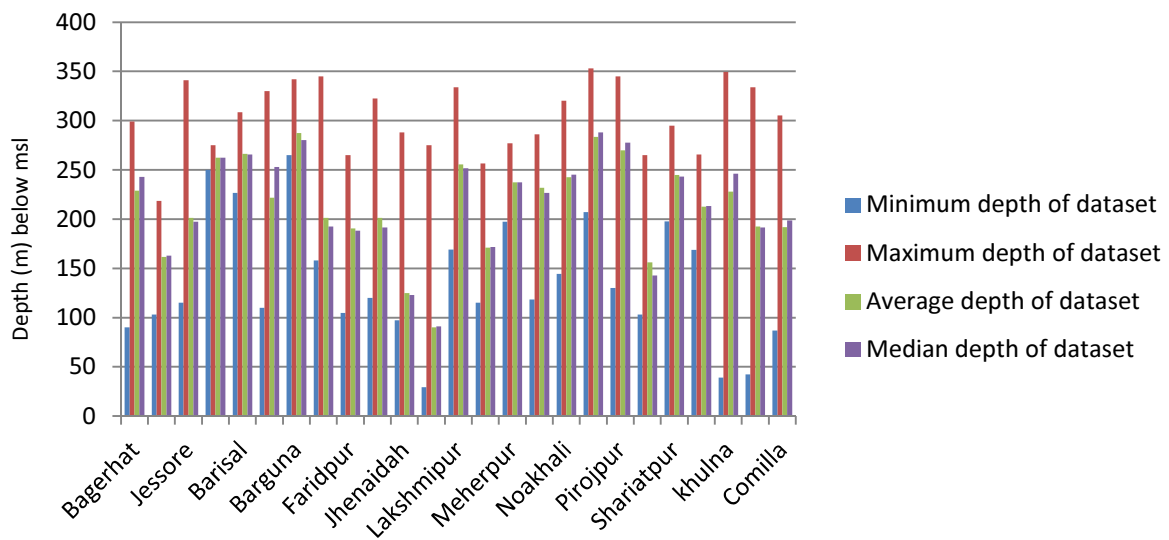Figure 2.15: DPHE minimum, maximum and average depths of abstraction.

Figure 2.16: Some statistics of the DPHE well depth dataset. The median and average depths are closely together for each district.

It is likely that the received information about well depths from DPHE only reflects a minor part of the wells, since drilling at these depths is very expensive (Escamilla et al., 2011). However, this data is still used to define depths, since other data sources are absent and literature only contains coarse averages with no information regarding the spatial distribution of well depths. Also the depths of this dataset correspond to the salinity profile established by BGS and DPHE (2001), which shows that the majority of the wells are located at those depths so that they abstract fresh water.

For the overview: 1) irrigation STW abstracts water between 10-60m depth, 2) irrigation DTW abstracts water between 60-100m depth and 3) domestic and industrial abstraction depths are based on the well data of DPHE (between minimum and maximum depth in each district).

2.4.4   Low permeability lithology

The hydrogeological cross-section of BGS and DPHE (2001) shows several low permeability layers (KH = 0.05m day^{-1}). It would make sense that abstraction does not occur in such layers. Therefore wherever a model cell has a value smaller than or equal to this horizontal conductivity value (0.05m day^{-1}), there is no abstraction in this cell. A horizontal conductivity higher than 0.005m day^{-1} does allow abstraction.

2.5 River bathymetry, water levels and salinity (RIV)

The river network shapefile delivered by CEGIS (red figure) does not cover the entire model area. River networks for the remainder part of the model domain were downloaded from the diva-gis[18] website. The resulting combined river network shapefile was converted to raster. This raster was adapted for locations where rivers were disconnected or the border between land and sea was not well defined. The resulting river cell grid can be seen in figure 2.17 (right).

Note: Of the following constructed river maps, only the information is used from these cells at locations where there are river cells assigned in the model (layers 1-5 model section 1). The remainder part of the cells reflects a general head boundary (figure 1.2) and uses other information.
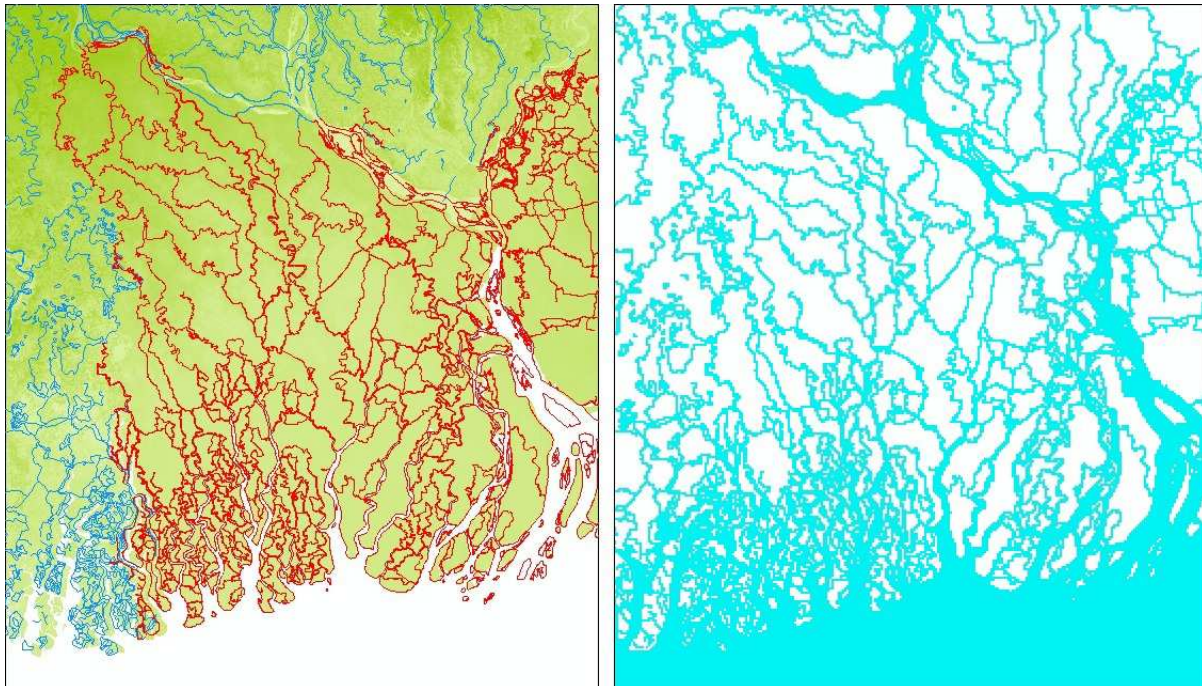

Figure 2.17: Left: Shapefile of the river network of CEGIS (red) and diva-gis (blue). Right: Rasterized shapefile now represents river cells.

2.5.1   River bathymetry

Cross-section data from BWDB (delivered by CEGIS) is available at 283 locations for a limited number of river reaches (figure 2.18 lower left). The river bottom elevation is determined by averaging the cross-section data per station for the period of 1990 and onwards (maximum of 2008). The stations only cover a few grid cells and their information needs to be interpolated to attain a river bottom elevation for the remainder river cells. However, an interpolation routine normally defines a value for every grid cell in a raster and not only a river grid cell i.e. it does not consider the border between land and water. Also, the connectivity of the river bed elevation between different tributaries is difficult to match. To avoid this problem we make use of the fact that a stream gradient follows the gradient of surface elevation. That is why the digital elevation map is used as a reference of the river bottom elevation. This DEM also contains bathymetry for the sea and estuaries. Because of the initially high resolution (5km) this DEM does not contain river bathymetry for the rivers, which generally have a smaller width than 5 km. Their depths cannot be detected anymore due to the

---

[18]http://www.diva-gis.org/gdata

averaging between cells during resampling and these depths are attained by comparing the river bottom elevation data of the stations and the digital elevation map.

The difference in elevation between the DEM and the measured river bottom elevation at the location of the stations is calculated (DEM-RBOT) (figure 2.18 upper). There was no spatial pattern in the difference between the DEM and the measured river bottom elevation at the stations. The average difference is 2.21m i.e. the DEM is on average 2.21m higher compared to the river bottom elevations. Differences with more than two standard deviation distance from the mean are discarded as outliers (green data points in figure 2.18). The average difference (2.21m) is subtracted from the digital elevation map to attain river bottom elevations. However, to avoid that the bathymetry of the sea and estuaries is wrongly affected, this difference is not subtracted in the Southern part of the model domain. This is defined as a border of 55km distance from the South border of the model domain (figure 2.18 lower left). In this area is the majority of the sea bottom bathymetry located. The corrected DEM which now represents the river bottom elevations is smoothly attached to the unadapted bathymetry.The river cells are filled with the associated values of the corrected DEM (figure 2.18 lower right).
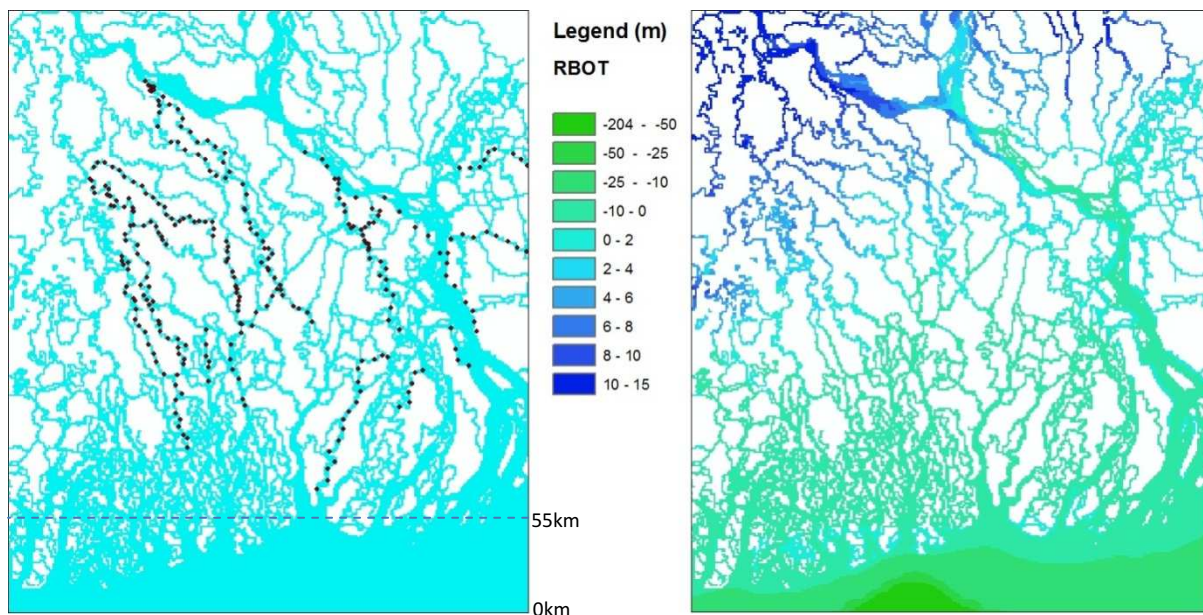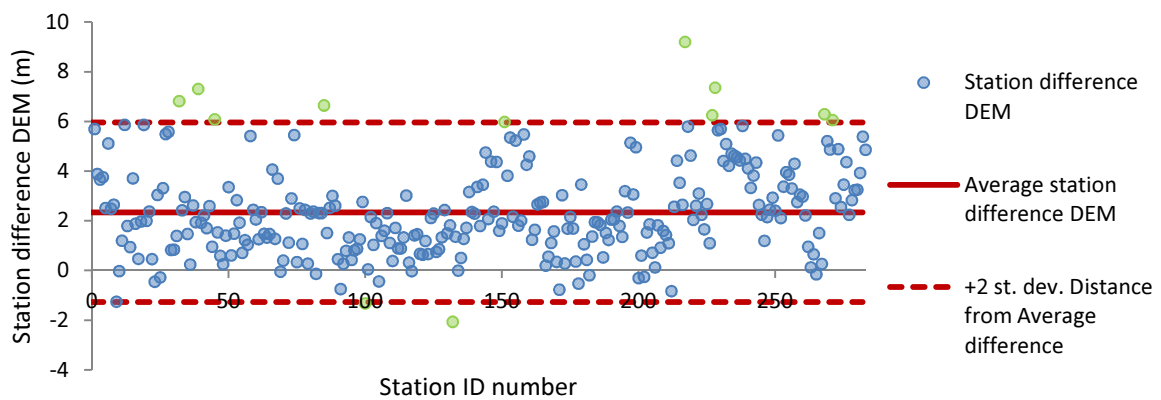

Figure 2.18: Upper: difference between the DEM and the river bottom elevation data at the 283 locations (station ID number). The outliers are also shown as green data points. Lower left: river raster with the locations of the stations. Lower right: Established river bottom elevation.

2.5.2 River water levels

The water level in every river cell is conducted the same way as the river bottom elevation, since the water level, just as the river bottom elevation, follows the gradient of the surface. The water level data is available at 126 locations (BWDB delivered by CEGIS) on a daily basis interval and includes a high tide and a low tide water level (figure 2.19). These water levels are averaged per station for the period of 1990 and onwards. However, at stations where there is little data in this period and at stations where there is no data of this period (older data present), the data used deviates from the 1990-onwards time period. The data is divided over the three stress periods, thus assigning three water levels to each station (figure 2.20). The third stress period of March-May is added, because snowmelt already affects discharge in this pre-monsoon period[19] (Jian et al., 2009). The average water level of all stations relative to the mean sea level is 1.36m, 1.38m and 2.62m for the period of November-February, March-May and June-October, respectively. The effect of melt water affecting discharge in the pre-monsoon period is not identified very clearly in this dataset.
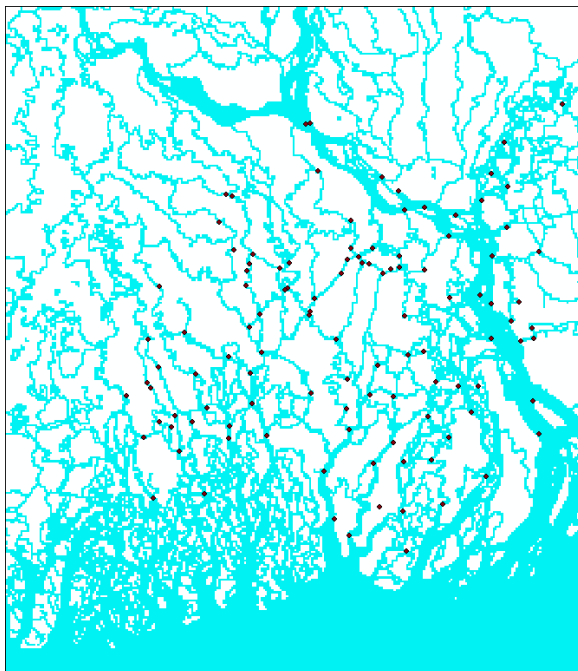

Figure 2.19: Locations of the water level stations on the river cell grid.

The average difference between the DEM and the water levels at the measurement locations can be seen in figure 2.20 (DEM - water level). The average differences are 1.40m, 1.37m and 0.12m for the first, second and third stress period respectively. As expected, the water levels have a lower difference with the DEM than the river bottom elevation. The difference between the first and second period is very low as already indicated by the approximately same average water levels. The low value of the third stress period indicates that water levels are close to the surface elevation. Every raster value in the DEM equal or smaller than the average difference is assigned zero. For example, the DEM in stress period 1 is on average 1.40m higher than the water level, thus subtracting 1.40m from the DEM grid cells, which have a cell value of 1.40 or smaller, equals sea level. The average difference is subtracted from the DEM when grid cell values are higher than the average difference. The river cells are then filled with the associated values of these three corrected DEM's (figure 2.20).

[19] http://www.eu-highnoon.org/case-studies/rainfallsnowmeltcontributionsdischargeganges
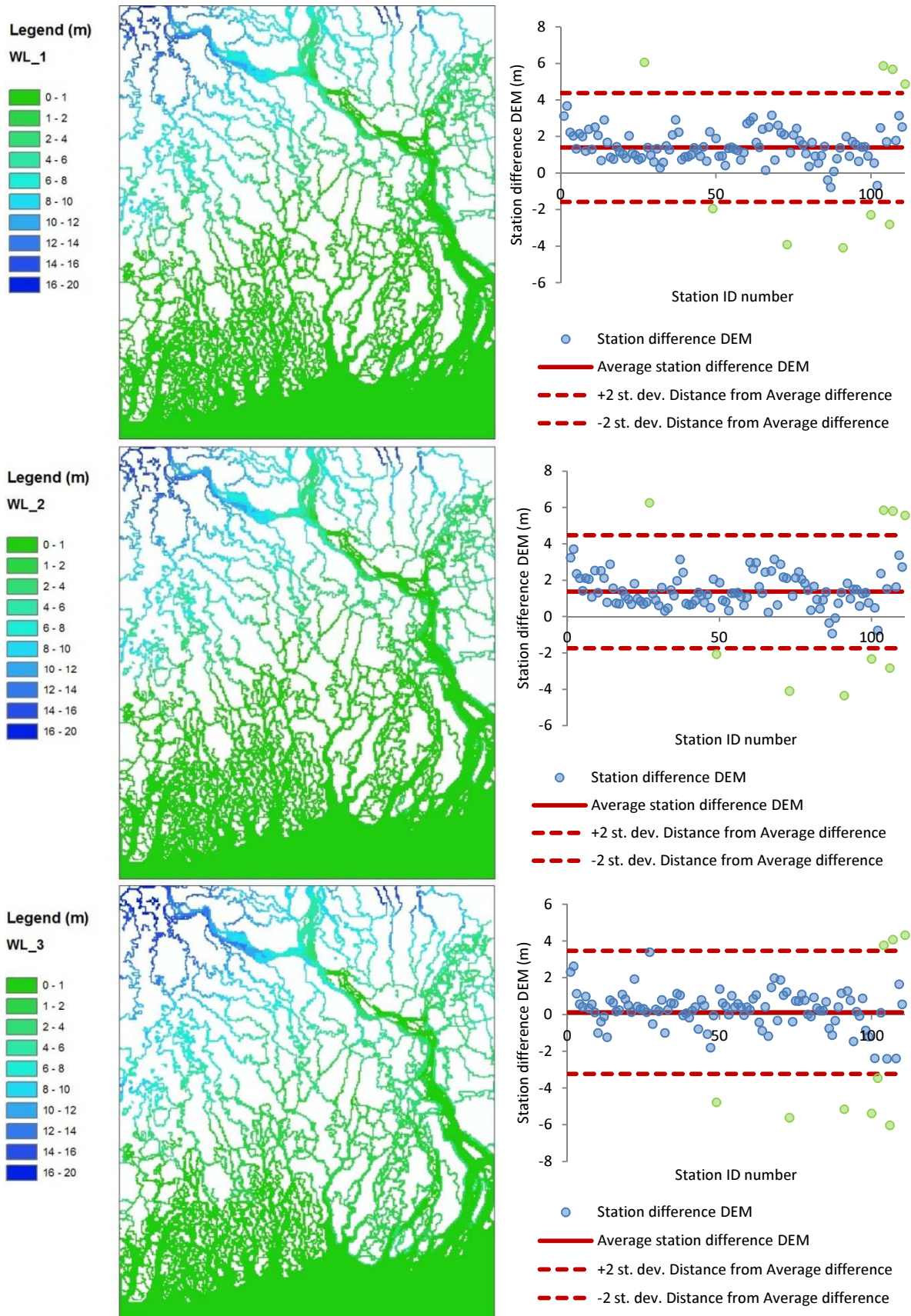
Figure 2.20: Water level maps for the three stress periods and their associated graphs, which show the difference between the DEM and the water level at each station. Green data points are discarded, because the distance from the average is more than two standard deviations.

2.5.3 River salinity (combined general head boundary),

There are surface EC and chlorinity values available at 84 locations measured by BWDB on a monthly basis (figure 2.21). At first instance the EC values were used to compare them with the groundwater EC values. Therefore these EC values are now used rather than the chlorinity values in further data processing. These values are averaged per station over the period of 1990 and onwards. These EC measurements are divided over the stress period, since the salinity is influenced by the amount of discharge (mixing of fresh water), which in turn depends on seasonality (2.5.2). The EC measurements are converted to salinity values (TDS) using two equations. The first one is the EC-Chloride relation according to De Louw et al. (2011):

$$Cl\ (g\ L^{-1}) = EC\ (mS\ cm^{-1}) * 0.36 - 0.45$$

Of this equation the lower bound of 0.36 is chosen, since the salinity of the northern part of the Bengal Basin is generally lower due to the large influx of fresh water. What follows is a conversion of the chloride concentration to salinity using the equation:

$$Salinity\ (g\ L^{-1}) = Cl^{-}(g\ L^{-1}) * 1.80665$$
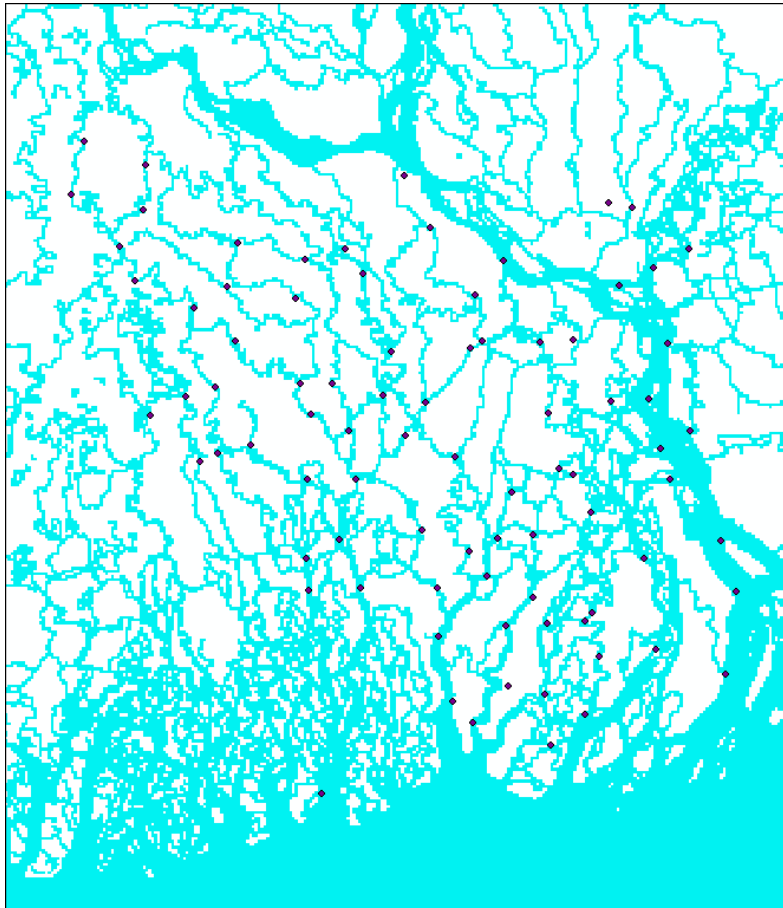
Figure 2.21: Locations of the 84 surface salinity measurement points in the area.

The distribution of the measurements (good spread) is such that interpolation is done over the entire raster, thus every grid cell is filled. The river cell raster is filled with these interpolated salinity rasters per stress period (figure 2.22). The result indeed shows that stress period 2 (March-May) has the highest salinity values, because the influx of fresh water is still relatively low and the hot temperatures stimulate evaporation. Apparently the melt water contribution to discharge is not

significant enough to really deflect salinity intrusion. Also salinity intrusion is less severe in the South-Eastern part of the model area, which highlights the relatively immense influx of fresh water from the Ganges compared to the other relatively minor rivers. Salinity is relatively low during the monsoon season (stress period 3), which is a result of the high influx of fresh water as expected. The salinity patterns are also pretty similar to the salinity maps established in the study of Winterwerp and Giardino (2012).
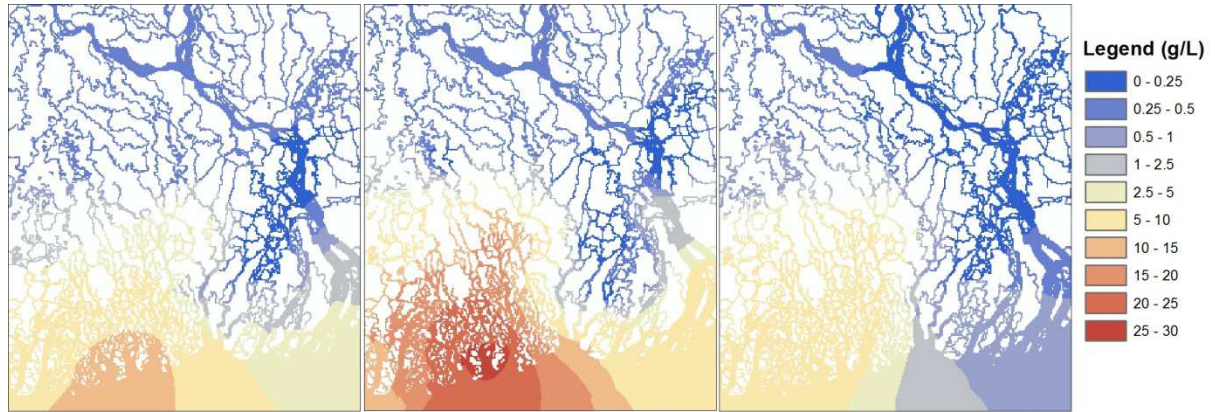

Figure 2.22: Established surface salinity maps for the three stress periods November-February, March-May and June-October respectively (left to right).

2.6 Precipitation and evapotranspiration (RCH)

Data of rainfall (BWDB), evaporation and evapotranspiration (BMD) have been delivered by CEGIS. Rainfall data is measured at 96 locations (figure 2.23) for the period 1961-2008 on a daily basis. Evaporation and evapotranspiration data is available for only 4 locations (figure 2.23) for a period of 1986-2011 (daily) and 1976-1998 (monthly) respectively[20]. The evapotranspiration rather than the evaporation data is used, since it also incorporates transpiration from vegetation. The evapotranspiration and rainfall data are divided over the three stress periods and averaged per station. Data measured before 1990 is discarded. Recharge rates will be determined by calculating the difference between rainfall and evapotranspiration i.e. the net product of rainfall after evapotranspiration. The point data needs to be interpolated to attain a value for every grid cell. This makes sense for the rainfall data, since there are enough points that can be used in the interpolation routine. However, for the evapotranspiration data, it would not make sense to interpolate an area of 274kmx317km based on 4 points. The resulting trends in evapotranspiration would be statistically meaningless. It was decided to use the average of the 4 stations per stress period for the whole model area, since the evapotranspiration data of the 4 stations do not differ much within each stress period (table 2.9). The precipitation and evapotranspiration data also contain data outside the model domain (figure 2.23). However this data is still incorporated in the average evapotranspiration calculations and in the interpolation routine for the rainfall data. This results in a better recharge representation at the borders of the model area. The concentration (TDS) of the recharge is set at zero.

	Station ID	$ET0_0$ mm day^{-1}
Stress period 1	11704	2,53
	11313	2,47
	11505	2,54
	11604	2,66
	Average	2,55
Stress period 2	11704	4,57
	11313	4,44
	11505	4,87
	11604	4,90
	Average	4,70
Stress period 3	11704	3,50
	11313	3,75
	11505	3,80
	11604	3,72
	Average	3,69

Table 2.9: Evapotranspiration data of the 4 stations per stress period and the average evapotranspiration used over the whole model domain per stress period.

---

[20] *Note: It is uncertain whether this is potential or actual evapo(transpi)ration. Since the project is momentarily on hold this might be clarified in the near future.*

Figure 2.23: Locations of rainfall measurements and evapo(transpi)ration measurements.

Rainfall rates (mm day^{-1}) can be seen in figure 2.24. Clearly the monsoon season (stress period 3) has the highest rates. The total recharge (rainfall – evapotranspiration) in the first stress period will be negative meaning that there is more evapotranspiration than rainfall. The total recharge in the second stress period will be partly positive and partly negative. The first and third stress period show an increasing rainfall trend in the NW-SE direction. This trend is in the second period directed from West to East.
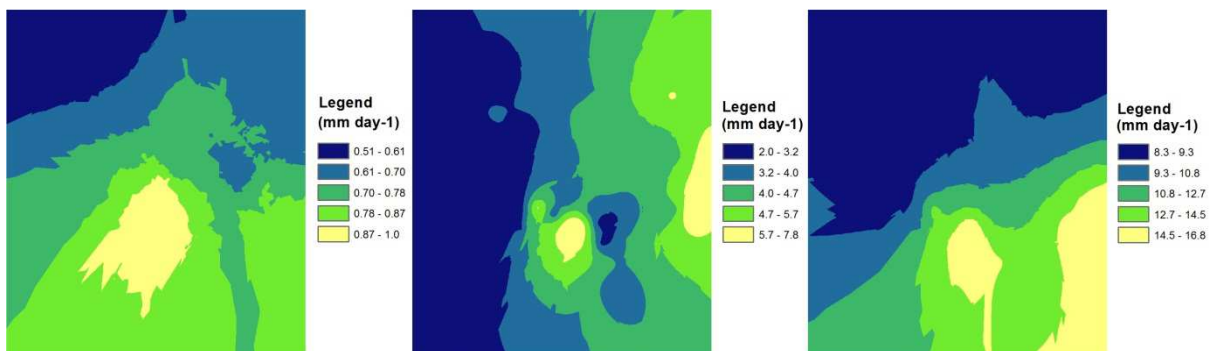

Figure 2.24: Rainfall rates (mm day^{-1}) for the first, second and third stress period respectively.

3. References

Benshila, R., Durand, F., Masson, S., Bourdallé-Badie, R., De Boyer Montégut, C., Papa, F., Madec, G., 2014. Ocean Modelling, Vol. 74, pp. 36 – 52.

BGS and DPHE, 2001. Arsenic contamination of groundwater in Bangladesh, Kinniburgh, D.G. and Smedley, P.L. (Editors), Volume 2: Final report, British Geological Survey Report WC/00/19, British Geological Survey, Keyworth, ISBN: 0 85272 384 9.

CIA (2006) The world fact book, US Central Intelligence Agency, Washington, DC. https://www.cia.gov/cia/publications/factbook/index.html). Cited April 2006

Davies, J., Herbert, R., 1990. Field determination of vertical permeability. British Geological Suvey Technical Report WD/90/47R.

De Louw, P.G.B., Eeman, S., Siemon, B., Voortman, B.R., Gunnink, J., Van Baaren, E.S., Oude Essink, G.H.P, 2011. Shallow rainwater lenses in deltaic areas with saline seepsage, Hydrol. Earth Syst. Sci., Vol. 15, pp. 3659 – 3678.

DPHE, GoB, APSU, JICA, 2006. Final report on development of deep aquifer database and preliminary deep aquifer map.

EPC/MMP, 1991. Dhaka region groundwater and subsidence study, Final report. Engineering and Planning Consultants, Dhaka and Sir M MacDonald and Partners, UK. Report for Dhaka Water Supply and Sewerage Authority under assignment to the World Bank.

Escamilla, V., Wagner, B., Yunus, M., Streatfield, P.K., Van Geen, A., Emch, M., 2011. Effect of deep tube well use on childhood diarrhoea in Bangladesh, Bulletin of the World Health Organization, Vol. 89, pp. 521 – 527.

Harvey CF, Ashfaque KN, Yu W, Badruzzaman ABM, M Ali A, Oates PM, Michael HA, Neumann RB, Beckie R, Islam S, Ahmed MF (2006) Groundwater dynamics and arsenic contamination in Bangladesh. Chem Geol 228:112–136

Hoque, M.A., 2010. Models for Managing the Deep Aquifer in Bangladesh, Unpublished Ph.D. Thesis, University College London, London, 265 pp.

Hoque, M., Burgess, W.G., 2012. 14C dating of deep groundwater in the Bengal Aquifer System, Bangladesh: implication for aquifer anisotropy, recharge sources and sustainability, Journal of Hydrology, Vol. 444 – 445, pp. 209 – 220.

Jian, J., Webster, P.J., Hoyos, C.D., 2009. Large-scale controls on Ganges and Brahmaputra river discharge on intra-seasonal and seasonal timescales, Q. J. R. Meteorol. Soc., Vol. 135, pp. 353 – 370.

Jones, P.H., 1985, Geology and groundwater resources of Bangladesh. P.H. Jones Hydrogeology Inc. World Bank (Asia Division).

Klump, S., Kipfer, R., Cirpka, O.A., Harvey, C.F., Brennwald, M.S., Ashfaque, K.N., Badruzzaman, A.B.M., Hug, S.J., Imboden, D.M., 2006. Groundwater dynamics and arsenic mobilization in

Bangladesh assessed using noble gases and tritium, Environmental Science Technology, Iss. 40, pp. 243 – 250.

Majumder, R.K., Halim, M.A., Saha, B.B., Ikawa, R., Nakamura, T., Kagabu, M., Shimada, J., 2011. Groundwater flow system in Bengal Delta, Bangladesh revealed by environmental isotopes, Environ. Earth. Sci., Vol. 64, pp. 1343 – 1352.

McArthur, J. M., Banerjee, D. M., Hudson-Edwards, K. A., Mishra, R., Purohit, R., Ravenscroft, P., Cronin, A., Howarth, R. J., Chatterjee, A., Talukder, T., Lowry, D., Houghton, S., Chadha, D. K., 2004. Natural organic matter in sedimentary basins and its relation to arsenic in anoxic ground water: the example of West Bengal and its worldwide implications. Appl. Geochem., Vol. 19, pp. 1255 – 1293.

Michael, H.A., Voss, C.I., 2009a. Estimation of regional-scale groundwater flow properties in the Bengal basin of India and Bangladesh, Hydrogeology Journal, Vol. 17, Iss. 6, pp. 1329 – 1346.

Michael, H.A., Voss, C.I., 2009b. Controls on groundwater flow in the Bengal Basin of India and Bangladesh: regional modeling analysis, Hydrogeology Journal, Vol. 17, Iss. 7, pp. 1561 – 1577.

MMI/HTS, 1992. Deep tubewell II project, final report, Natural resources, Vol. 2.1. Mott MacDonald Ltd. And Hunting Technical Services Ltd. Bangladesh Agricultural Development Corporation.

Mondal, M.S., Saleh, A.F.M., 2003. Evaluation of some deep and shallow tubewell irrigated schemes in Bangladesh using performance indicators, Agricultural Water Management, Vol. 58, Iss. 3, pp. 193 – 207.

Morton, W.H., Khan, Q., 1979. Groundwater in the coastal zone and offshore islands of Bangladesh.

MPO, 1987. The groundwater resource and its availability for development, Technical report No. 5, Master Plan Organization, Ministry of Water Resources, Government of Bangladesh. Harza Engineering USA in association with Sir MacDonald and Partners, UK, Met Consultants, USA and EPC Ltd, Dhaka.

Mukherjee, A., Fryar, A. E., and Howell, P. D.: Regional hydrostratigraphy and groundwater flow modeling in the arsenic affected areas of the western Bengal basin, West Bengal, India, Hydrogeol. J., 15(7), 1397–1418, doi:10.1007/s10040-007- 0208-7, 2007.

Rahman, A.A. and Ravenscroft, P., 2003. Groundwater Resources and Development in Bangladesh, Chapter 23, Options for Arsenic Removal from Groundwater, Firoz Mallick, A.S.M. and Hirendra Kumar Das, The University Press Limited, 2003. BADC, 2011

UNDP, 1982. Groundwater Survey: The Hydrogeological Conditions of Bangladesh. UNDP Technical Report DP/UN/BGD – 74 – 009/1, 113 pp.

Winterwerp, J.C., Giardino, A., 2012. Assessment of increasing freshwater input on salinity and sedimentation in the Gorai river system, Deltares, Netherlands.

WARPO (Water Resources Planning Organization) (2000) National Water Management Plan Project: draft development strategy. Ministry of Water Resources, Government of the People's Republic of Bangladesh, Dhaka

4. Appendices

4.1 Model layer overview

Layer	Depth
(1)	15m
(2)	10m
(3)	5m
(4)	0m
(5)	-5m
(6)	-10m
(7)	-15m
(8)	-20m
(9)	-25m
(10)	-30m
(11)	-35m
(12)	-40m
(13)	-45m
(14)	-50m
(15)	-55m
(16)	-60m
(17)	-65m
(18)	-70m
(19)	-75m
(20)	-80m
(21)	-85m
(22)	-90m
(23)	-95m
(24)	-100m
(25)	-105m
(26)	-115m
(27)	-125m
(28)	-150m
(29)	-175m
(30)	-200m
(31)	-225m
(32)	-250m
(33)	-275m
(34)	-300m
(35)	-400m
(36)	-500m
(37)	-1000m
(38)	-1500m
(39)	-2000m
(40)	-2500m
	-3000m

4.2 Hydrogeological cross-section for model domain (upper 300m)
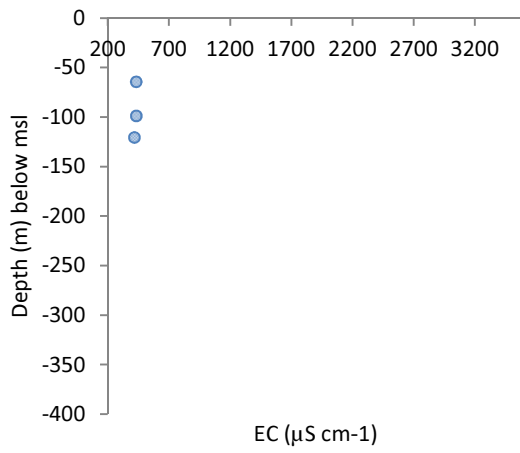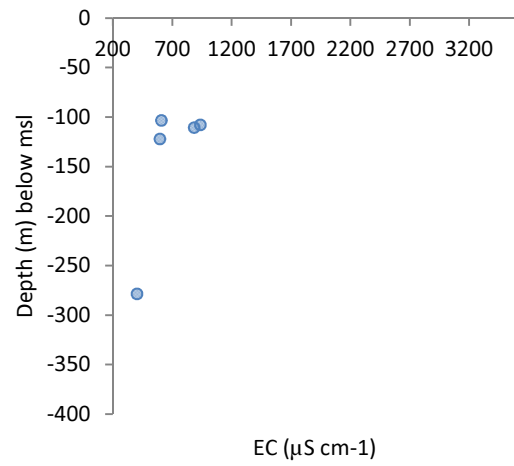
Delta system and Coastal belt
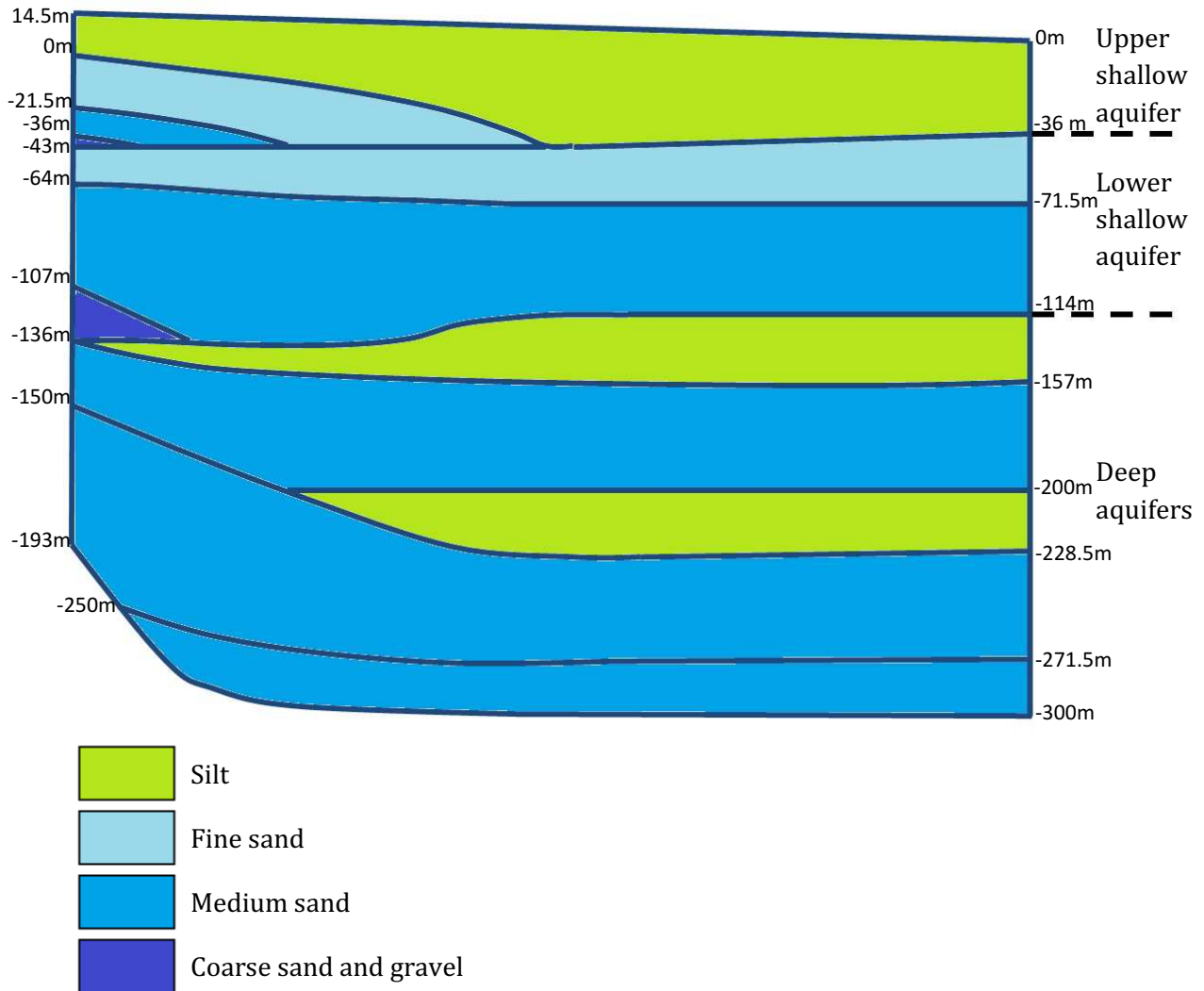
Adapted from BGS and DPHE (2001)
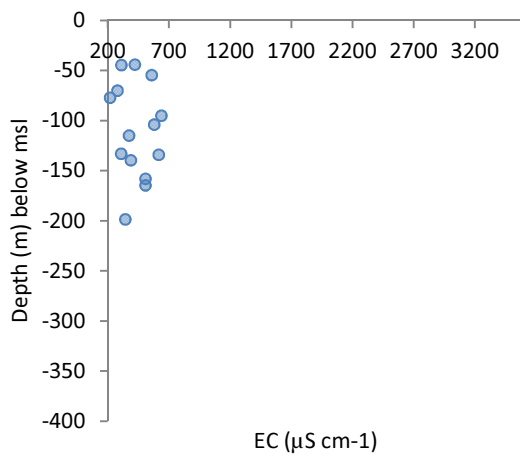
4.3 Groundwater EC data (DPHE)

01-002

01-006

01-009

02-001

02-002

02-003

02-005

02-006

03-002

03-008

05-002

05-003

05-005

05-008

05-009

05-011

02-008